Endocytosis frustration potentiates compression-induced receptor signalling

Francesco Baschieri, Dahiana Le Devedec, Samuel Tettarasar, Nadia Elkhatib, Guillaume Montagnac

Title:

Endocytosis frustration potentiates compression-induced receptor signalling

Authors:

Francesco Baschieri[1*], Dahiana Le Devedec[1*], Samuel Tettarasar[1], Nadia Elkhatib[1], and Guillaume Montagnac[1]

Affiliations:

[1] Inserm U1279, Gustave Roussy Institute, Université Paris-Saclay, Villejuif, France

* These authors contributed equally

Corresponding authors: guillaume.montagnac@gustaveroussy.fr;

francesco.baschieri@gustaveroussy.fr

Abstract:

Cells experience mechanical stresses in different physiological and pathological settings. Clathrin-coated structures (CCSs) are sensitive to such perturbations in a way that often results in a mechanical impairment of endocytic budding. Compressive stress is a mechanical perturbation that leads to increased membrane tension and promotes proliferative signals. Here, we report that compression leads to CCSs frustration and that CCSs are required to potentiate receptor-mediated signaling in these conditions. We show that cell compression stalled CCSs dynamics and slowed down the dynamic exchange of CCSs building blocks. As previously reported, compression-induced paracrine activation of the epidermal growth factor receptor (EGFR) was the primary cause of ERK activation in these conditions. We observed that the EGFR was efficiently recruited at CCSs upon compression and that CCSs were required for full ERK activation. In addition, we demonstrated that compression-induced frustrated CCSs could also increase ligand-dependent signaling of other receptors. We thus propose that CCS frustration resulting from mechanical perturbations can potentiate signaling through different receptors with potential important consequences on cell adaptation to its environment.

Main Text:

INTRODUCTION

Clathrin-mediated endocytosis (CME) relies on the assembly of clathrin-coated structures (CCSs) at the internal leaflet of the plasma membrane. CCSs are endowed with the capacity to recruit specific receptors and to bend the membrane in order to generate receptor-containing endocytic vesicles (McMahon and Boucrot, 2011). Membrane bending is however sensitive to mechanical perturbations that oppose the invagination force generated by CCSs. For instance, high plasma membrane tension stalls CCSs invagination and thus prevents CME (Boulant et al., 2011; Raucher and Sheetz, 1999). Other types of mechanical perturbations can also prevent normal CCSs budding. For example, a subset of CCSs termed tubular clathrin/AP-2 lattices (TCALs) that specifically nucleate at cell/collagen fibers contact sites show reduced dynamics because they try and fail to internalize fibers that are longer than the cell itself (Elkhatib et al., 2017). High substrate rigidity can also impair CCSs budding through favoring the αvβ5 integrin-dependent formation of flat and long-lived clathrin-coated plaques (Baschieri et al., 2018). Thus, CCSs frustration is a common response to a wide array of mechanical perturbations. CCSs frustration may not simply be a passive consequence of environmental perturbations but could actually participate in building an adapted response to these modifications. Indeed, we showed that TCALs help the cell to migrate in 3D environments (Elkhatib et al., 2017) and that clathrin-coated plaques that assemble on stiff substrates serve as signaling platforms for different receptors, ultimately leading to sustained cell proliferation (Baschieri et al., 2018).

Cell compression was recently shown to induce CCSs frustration as well, most likely because of an increased membrane tension (Ferguson et al., 2017). Compressive forces are frequently encountered in the organism, whether in a physiological or pathological context (Butcher et al.,

2009; Kalli and Stylianopoulos, 2018; Nia et al., 2017; Rakesh et al., 2010; Tschumperlin et al., 2004). These forces deeply impact the cell physiology and modulate signaling pathways as well as gene expression profile. For example, in bronchial epithelial cells, compression was shown to activate the epidermal growth factor receptor (EGFR) through a force-induced, metalloprotease-dependent shedding of HB-EGF precursor (Tschumperlin et al., 2004). In addition, mechanical compression in solid tumors was reported to promote both proliferation and apoptosis via mechanisms that are still not entirely clear (Alessandri et al., 2013; Cheng et al., 2009). Yet, whether compression-induced EGFR activation (Tschumperlin et al., 2002; Tschumperlin et al., 2004) is at stake in tumors is not known. Because we previously observed that the EGFR uses frustrated clathrin-coated plaques as signaling platforms (Baschieri et al., 2018), we wondered whether pressure-induced CCSs frustration could participate in EGFR signaling in these conditions.

RESULTS

Compression reduces CCS dynamics

To investigate the consequences of compressive forces on CCSs dynamics, we used HeLa cells that were genome-edited to express a fluorescently-tagged version of µ2-adaptin, a subunit of the clathrin adaptor AP-2 (Fig. S1a-c). Cells were grown on glass coverslips and confined under an agarose plug under a constant compressive stress of 1 kPa (see materials and methods and Fig. S1d) that closely match the reported stress observed in solid tumors (between 0.21 to 20 kPa in tumors; negligible in healthy tissues) (Fernández-Sánchez et al., 2015; Kalli and Stylianopoulos, 2018; Nia et al., 2017). We noticed that confinement induced an enlargement of the cell area and blebs were often observed at the cell edges (Fig. S1e), suggesting that membrane tension is most likely dramatically increased in these conditions (Gauthier et al., 2012). In addition, the nuclei of cells under compression were enlarged and nuclear blebs were also visible at their rim (Fig. S1f). These observations indicate that cells are indeed experiencing compression in our assays. Because compression stress higher than 3.87 kPa were reported to increase apoptosis in tumor spheroids in vitro (Cheng et al., 2009), we tested whether a transient solid stress of 1 kPa could modulate apoptosis or proliferation rates and found no significant differences before or after compression (Fig. S1g and h). In classical culture conditions, HeLa cells display a mixture of dynamic, diffraction limited CCSs, corresponding to canonical clathrin-coated pits, and long-lived, large CCSs, corresponding to clathrin-coated plaques. We observed that compression globally increased the lifetime of CCSs as well as the occurrence of plaques (as defined by a lifetime >300s; Fig. 1a and b), thus confirming previous reports (Ferguson et al., 2017). Because integrin αvβ5, which is necessary for clathrin-coated plaque assembly, could possibly play a role in pressure-induced global increase of CCSs lifetime, we treated cells with Cilengitide, a potent αvβ5 inhibitor. While

CCSs were mostly dynamic in Cilengitide-treated cells before pressure, confinement under the agarose gel dramatically increased the lifetime of CCSs as well as the occurrence of stalled CCSs (Fig. 1a and c). These results indicate that CCSs increased lifetime/stabilization under compression is independent of αvβ5 integrin and is most likely the consequence of increased membrane tension. Membrane tension was recently shown to regulate the dynamics of CCSs components (Bucher et al., 2018). To investigate whether pressure also impacts on the dynamics of major CCSs building blocks in our system, we performed fluorescence recovery after photobleaching (FRAP) experiments in cells expressing GFP-tagged μ2-adaptin. We chose to FRAP large and long-lived individual CCSs corresponding to clathrin-coated plaques because the long-lived nature of these structures allows to monitor fluorescence recovery over minutes. In control conditions, fluorescence recovery was fast (half-time recovery, t1/2 ≈ 8s) with a plateau reaching approximately 80%, thus showing that only ~20% of AP-2 complexes were immobile at CCSs (Fig. 1d and e). However, the mobile fraction only reached approximately 60% and half-time recovery was delayed when pressure was applied on cells (t1/2 ≈ 15s; Fig. 1d and e). Although we cannot strictly exclude that FRAP parameters may be affected by vesicular budding (Chen et al., 2019), these results suggest that cell compression slows down AP-2 turnover in a similar manner as increased membrane tension (Saleem et al., 2015).

Compression leads to CCSs-dependent EGFR signaling

Compressive forces have been reported to activate EGFR and downstream ERK signaling (Tschumperlin et al., 2002; Tschumperlin et al., 2004). Indeed, we observed that compression triggered transient ERK activation (Fig. 2a and b). Similar observations were made in cells experiencing a hypo-osmotic shock, a condition known to increase membrane tension (Fig. S2a

and b). Compression of three different transformed cell lines also led to transient ERK activation (Fig. 2c and d). We also observed that GFP-tagged ERK transiently translocated from the cytoplasm to the nucleus when HeLa cells were confined under the agarose plug thus confirming the activated status of ERK in these conditions (Fig. S2c and d). Pressure-induced ERK activation was dependent on EGFR expression (Fig. 2e and f and Fig. S2e) as well as on EGFR kinase domain activity as treatment with the EGFR kinase activity inhibitor Gefitinib inhibited ERK phosphorylation under compression (Fig. 2g and h).

CCSs have been shown to act as platforms that potentiate receptor-mediated signaling, particularly in the case of the EGFR (Sigismund et al., 2008; Vieira et al., 1996). Modulation of CCSs lifetime is an important regulator of receptor signaling output and for instance, long-lived clathrin-coated plaques are more potent than dynamic clathrin-coated pits in supporting signaling (Baschieri et al., 2018). Because compression stalls CCSs dynamics, we reasoned that compression-induced ERK activation could be at least partially due to the increased lifetime of CCSs induced by mechanical stress. Indeed, we observed that AP-2 subunits or clathrin heavy chain (CHC) knockdown reduced ERK activation under compression (Fig. 2i and j and Fig. S2e). Thus, CCSs are required for full EGFR signaling in compressed cells.

Mechanisms of EGFR recruitment at frustrated CCSs under pressure

EGFR is recruited to CCSs upon ligand-induced activation (Rappoport and Simon, 2009). To ascertain whether compressive stress would lead to the same outcome, genome-edited HeLa cells expressing mCherry-tagged, endogenous μ2-adaptin and overexpressing GFP-tagged EGFR were compressed under an agarose plug and monitored using total internal reflection fluorescence (TIRF) microscopy. EGFR quickly accumulated at CCSs upon compression (Fig. 3a and b, Video

1). Increasing membrane tension through applying a hypotonic shock on cells also resulted in EGFR recruitment at CCSs (Fig. S3a and b). We also observed a punctuated phospho-tyrosine staining colocalizing with CCSs in cells experiencing compression (Fig. S3c and d). This staining was specifically lost in cells pretreated with Gefitinib (Fig. S3c and d) suggesting that activated EGFR is present at CCSs in control cells under compression. Surprisingly, Gefitinib did not prevent the compression-induced EGFR accumulation at CCSs (Fig. 3b and c, Video 2). This latter observation is in favor of a previously proposed model whereby ligand-induced EGFR dimerization is required to interact with the CCS machinery, in a kinase domain activity-independent manner (Wang et al., 2005).

Of note, all these experiments were performed in the absence of serum and of any added EGFR ligands. It has been reported that, in bronchial epithelial cells, the compression resulting from bronchoconstriction induces an ADAM metalloprotease-dependent EGF-family ligand heparin-binding EGF (HB-EGF) ectodomain shedding, thus leading to para-autocrine EGFR stimulation (Tschumperlin et al., 2004). Inactivation of these metalloproteases using the large spectrum metalloprotease inhibitor Batimastat was shown to prevent EGFR activation following compressive stress (Tschumperlin et al., 2004). Indeed, we observed that Batimastat reduced both EGFR recruitment at CCSs (Fig. 3b and d, Video 2) and ERK activation (Fig. 3e and f) upon compression. Conditioned medium from compressed cells was sufficient to activate ERK in serum-starved cells (Fig. S3e and f). However, conditioned medium from compressed cells treated with Batimastat failed to activate ERK (Fig. S3e and f). Of note, Batimastat did not inhibit ERK activation when EGFR was stimulated using externally added EGF (Fig. S3g and h). We hence subjected Batimastat-treated cells to hypotonic swelling to increase their plasma membrane tension and observed that Batimastat treatment prevented EGFR recruitment to CCSs in these conditions

(Fig. S3a and b). Together, in agreement with the literature, our data suggest that cellular compression leads to metalloprotease-dependent shedding of EGFR ligands, thus resulting in EGFR activation.

Compression-induced CCSs frustration modulates receptor sorting

Frustration of the endocytic machinery could potentially impact any CCS cargo. We therefore aimed at determining whether other receptors could also be recruited at CCSs upon cell compression. We first analyzed the dynamics of the prototypical CCS cargo transferrin receptor (TfR) that is usually constitutively recruited at CCSs in order to be internalized. While mCherry-tagged TfR strongly accumulated at CCSs in control cells, it was excluded from CCSs in compressed cells (Fig. 4a and b, Video 3). This surprising results suggest that compression modulates receptor sorting at CCSs. Given that EGFR accumulates in CCSs of compressed cells, we sought to test if EGFR and TfR competed for their recruitment to CCSs, despite having different sorting motifs (Bonifacino and Traub, 2003). However, TfR was still excluded from CCSs of compressed cells upon EGFR knockdown, showing that no competition exists between these two receptors (Fig. 4b). We also observed a global increased of plasma membrane TfR-associated signal upon compression (Fig. 4c and Video 3). This most likely reflects the dramatic inhibition of TfR uptake from the cell surface, leading to its accumulation at the plasma membrane. In addition, we observed in FRAP experiments that fluorescence recovery of EGFR-GFP at CCSs was reduced in cells experiencing compression as compared to uncompressed cells stimulated with 10 ng/ml EGF (Fig. S4a). Thus, compression impacts on both CCS component dynamics (Fig. 1d) and CCS cargo dynamics (Fig. 4a and b and Fig. S4a). We next looked at different receptors whose endocytosis is normally triggered by their ligands. G-protein coupled receptor (GPCR)

Angiotensin receptor-1 (AT1R), as well as hepatocyte growth factor receptor (HGFR) that are recruited at CCSs upon specific ligand stimulation (Fig. S4b and c) (Eichel et al., 2016; Petrelli et al., 2002) did not accumulate at CCSs under pressure in the absence of ligands (Fig. 4d and e). These results indicate that compression does not result in the fast activation of these receptors in the absence of their specific ligands.

Compression-induced CCSs frustration controls signaling

We reasoned that, beside the specific case of EGFR, frustrated CCSs could have an impact on signaling downstream of other receptors, provided that receptors' ligands are present in the system. To test this hypothesis, we incubated HeLa cells in medium supplemented with suboptimal doses of either HGF or Angiotensin II and tested consequences on HGFR or AT1R localization, respectively. None of the two receptors accumulated at CCSs in these non-acute stimulation conditions (Fig. 5a-d). However, cell compression led to an efficient recruitment of these receptors at CCSs (Fig. 5a-d). Receptors clustering at CCSs most likely results from low levels of receptors activation, leading to their progressive accumulation at compression-induced frustrated CCSs. In addition, Gefitinib-mediated inhibition of EGFR was not sufficient to block ERK activation in compressed cells treated with suboptimal doses of HGF (Fig. 5e and f). This demonstrates that, provided the appropriate ligand is present, receptors other than EGFR can be trapped in compression-induced frustrated CCSs, thus leading to sustained signaling in the ERK pathway.

DISCUSSION

Here, we confirmed previous findings showing that cell compression leads to frustrated endocytosis, with an accumulation of long-lived CCSs (Ferguson et al., 2017). Several pieces of

evidence point to a predominant role of integrins in CCSs frustration through local anchoring of the CCSs machinery to the substrate (Baschieri et al., 2018; De Deyne et al., 1998; Elkhatib et al., 2017). HeLa cells display numerous frustrated CCSs, also termed clathrin-coated plaques, whose formation depends on local enrichment of the αvβ5 integrin (Baschieri et al., 2018). Yet, inhibiting this integrin did not prevent the accumulation of long-lived CCSs in cells experiencing compression. Cell compression most likely results in a dramatic increase in membrane tension that is known to impede CCSs budding (Boulant et al., 2011; Raucher and Sheetz, 1999). Thus, our data strongly suggest that CCSs frustration, as detected in compressed cells, results from increased membrane tension.

We also reported that AP-2 dynamics is perturbed at frustrated CCSs under compression. This may also result from increased membrane tension as this feature is known to modulate CCS components interaction with the plasma membrane (Saleem et al., 2015). Altered dynamics of CCS components is likely to perturb cargo recruitment at CCSs and, indeed, we observed that the TfR is excluded from CCSs under compression. It is not clear why some receptors like EGFR, HGFR, and AT1R can still be recruited at compression-induced frustrated CCSs upon ligand binding, while the TfR, which is normally constitutively addressed to these structures becomes excluded. This may depend on the different types of endocytosis motifs present on receptor cytosolic tails that engage different recognition sites on the AP-2 complex and/or on other CCSs components (Bonifacino and Traub, 2003). In addition, it remains to be elucidated why the dynamics of EGFR is reduced at compression-induced frustrated CCSs. It is possible that the reduced AP-2 dynamics we observed at frustrated CCSs modulates interactions between cargos and the clathrin coat. Along this line, it was recently shown that clathrin dynamic exchange at CCSs is critical to regulate cargo sorting (Chen et al., 2019).

It was previously reported that EGFR becomes activated in bronchial epithelial cells subjected to mechanical stress, leading to strong ERK activation. This activation was shown to be dependent on metalloprotease-regulated HB-EGF shedding and on the reduction of the intercellular space leading to paracrine activation of the receptor (Tschumperlin et al., 2004). Our data demonstrate that a similar mechanism exists in different transformed cell lines, suggesting that compression-induced EGFR activation could play an important role in physiophatological situations like solid tumors that are often characterized by high mechanical pressure. Opposed to what was described for bronchial epithelial cells, cancer cells responded to the soluble factor even in non-constricted environments (Fig S3e and f), suggesting that a reduction of intercellular space is dispensable in our model. Surprisingly, we observed that EGFR recruitment at CCSs does not depend on the activity of the kinase domain of the receptor. It has long been believed that EGFR autophosphorylation is required for both signaling output and endocytosis of the receptor (Lamaze and Schmid, 1995). Yet, some studies have suggested that ligand-induced EGFR dimerization is sufficient to induce the accumulation of the receptor at CCSs, without the need for autophosphorylation of the cytosolic tail (Wang et al., 2002; Wang et al., 2005). Our data clearly support this model.

We additionally showed that CCSs are required for full ERK activation downstream of the EGFR in compressed cells. These observations are in good agreement with previous reports demonstrating that CCSs can serve as signaling platform for EGFR (Sigismund et al., 2008; Vieira et al., 1996). Yet, we previously demonstrated that clathrin-coated plaques can also serve as signaling platform for other receptors (Baschieri et al., 2018). Here, we report that compression-induced frustrated CCSs can potentiate HGFR signaling when HGF is present in the extracellular environment, leading to strong ERK activation even when EGFR kinase activity is inhibited. It is

likely that frustrated CCSs trap the few activated HGFRs that, instead of being internalized, progressively accumulate in these stalled structures. The same holds true for AT1R, raising the possibility that this might be a general mechanism concurring to potentiate signaling in cells that experience solid stress. This is of special interest in the case of cancer, where cells are often subjected to mechanical stress in an environment that is rich in several growth factors (Shojaei et al., 2010; Straussman et al., 2012; Zhang et al., 2010).

To conclude, we propose that, in complex microenvironments, mechanical stress leads to the activation of the ERK signaling pathway not only because of HB-EGF shedding and paracrine activation of the EGFR, but also because compression-induced frustrated CCSs can trap and potentiate signaling by many other receptors.

METHODS

Cell lines and constructs

HeLa cells (a gift from P. Chavrier, Institut Curie, Paris, France; ATCC CCL-2), genome-edited HeLa cells engineered to expressed an endogenous GFP-tagged or mCherry-tagged µ2 subunit, HepG2 cells (ATCC HB-8065), Caco-2 cells (ATCC HTB-37), Hs578t cells (a gift from C. Lamaze, Institut Curie, Paris, France), were grown in DMEM Glutamax supplemented with 10% foetal calf serum at 37°C in 5% CO2. For microscopy, cells were serum-starved for at least 2h before the experiment. All cell lines have been tested for mycoplasma contaminations. mCherry-TfR was a gift from Michael Davidson (Addgene plasmid #55144). GFP-ERK2 was a gift from Dr.Hesso Farhan. EGFR-GFP was a gift from Alexander Sorkin (Addgene plasmid # 32751). pLenti-MetGFP was a gift from David Rimm (Addgene plasmid # 37560). AT1R-YFP was a kind gift of Dr. Mark Scott (Institut Cochin, Paris, France).

Plasmids were transfected 24h after cell plating using either Lipofectamine 3000 according to the manufacturer's instructions or electroporating cells in suspension using AMAXA nucleofector Kit V according to the manufacturer's instructions. Alternatively, linear Polyethylenimine (PEI - MW 25.000 – Polysciences Cat. Nr. 23966) at 1 mg/ml was used to transfect 50 % confluent cells in a 6 well plate according to the following protocol: 2 µg of DNA were added to 100 µl of OptiMEM, followed by addition of 4 µl of PEI, vortex and incubation for 10 minutes at RT prior to add the mix to the cells.

Antibodies and drugs

Rabbit polyclonal antibodies anti tot-ERK1/2 (Cat. Nr. 9102) and P-ERK1/2 (Cat. Nr. 9101) were purchased from Cell Signalling. Mouse monoclonal anti tot-ERK1/2 (Cat. Nr. 13-6200) was

purchased from Thermo Fisher. Mouse monoclonal anti-α-Tubulin (Cat. Nr. T9026) was purchased from Sigma. Mouse monoclonal anti-clathrin heavy chain (CHC, Cat. Nr. 610500) was purchased from BD Biosciences. Mouse monoclonal anti-α-adaptin (Cat. Nr. ab2807), rabbit monoclonal AP2M1 (Cat Nr. Ab75995) and rabbit monoclonal anti-EGFR (Cat. Nr. ab2430) were purchased from Abcam. Rabbit polyclonal anti-α-adaptin antibodies (M300) was purchased from Santa Cruz Biotechnology Inc. (Santa Cruz, CA, USA). Anti P-Tyrosine (Cat. Nr. 05-321) was obtained from Millipore. AnnexinV-Cy5.5 was from BD Biosciences (Cat nr. 559935). Antibodies used for western-blot analyses were diluted at 1:1000 in PBS-0.1% Tween-5% BSA or 5% non-fat dried milk. For immunofluorescences, antibodies were diluted 1:200 in PBS-0.3% BSA. HRP-conjugated anti-mouse and anti-rabbit antibodies for western-blot were from Jackson ImmunoResearch Laboratories (West Grove, PA, USA) and were used at a dilution of 1:3000. Alexa-conjugated antibodies as well as Cy3 and Cy5-conjugated antibodes were from Molecular Probes (Invitrogen) and were used at a dilution of 1:200.Gefitinib (Cat. Nr. CDS022106) was purchased from Sigma and used at a final concentration of 10 µM. Cilengitide was purchased from Selleckchem (Cat. Nr. S7077) and used at a final concentration of 10 µM. Human recombinant HGF (Cat. Nr. 1404 – used at 100 ng/ml), Human recombinant EGF (Cat. Nr. E9644 – used at 10 ng/ml), and Angiotensin II (Cat Nr. A9525) were purchased from Sigma. For HGF experiments in Fig 5a and b, cells were previously serum-starved for at least 2h and HGF was added to the serum-free medium for 1h before experiment. For AT1R experiments in Fig 5c, d cells were serum starved for 2h, then 1pM AngII was added for 5h in serum free medium prior to start the experiment. Sir-DNA (Spirochrome sc-007) was used at 0.5 µM to stain nuclei for live cell imaging. Cells were incubated for 20 minutes in the presence of Sir-DNA, then washed once with PBS to eliminate excess Sir-DNA and put back in DMEM.

In vitro compression experiments

To investigate the effect of compressive stress on cell behavior, an under-agarose assay was used (Heit and Kubes, 2003). Cells were plated either in 6-well cell culture plates or in glass-bottom dishes (µ-Dish Cat Nr 190301, Ibidi). 24h hours later, cells were subjected to mechanical stress by using an agarose plug overlaid with the weight necessary to reach a pressure of approximately 1000 Pa (agarose plug of 1.9 cm^2, corresponding to the area of one well of a 24-well, and weight of 20 g). To prepare agarose gels, agar was weighted and dissolved in DMEM Glutamax to a final concentration of 2.4%. The mixture was then cast in an empty dish or well and cooled at room temperature. Agar disks were sterilized under UV light and equilibrated at 37°C before use. For western blots, cells were subjected to compression for 30 minutes prior to cell lysis, unless otherwise stated. For video microscopy, videos were started 30 sec before applying the compressive stress. Compressed cells were then imaged for 30 min acquiring one image every 10 sec unless stated differently. Alternatively, for CCSs dynamics and for FRAP experiments, videos were acquired before and under compression and the videos before compression were compared to the videos under compression. For ERK2 and YAP nuclear enrichment, cells were treated with Sir-DNA as described above and imaged by spinning disk microscopy. Cells were manually segmented in FIJI and the Sir-DNA channel was used for the segmentation of the nucleus. Cytoplasm segmentation was obtained by subtracting the nucleus area from the cell area. ERK or YAP fluorescence was measured over time in the nucleus and in the cytoplasm, then the nuclear enrichment (nuclear/cytosolic signal ratio) was calculated for each cell.

Western Blots

For Western Blot experiments, cells were lysed in ice cold MAPK buffer (100mM NaCl, 10 nM EDTA, 1% IGEPAL ® CA-630, 0.1% SDS, 50mM TRIS-HCl pH 7.4) supplemented with protease and phosphatase inhibitors. Protein concentration was measured with Pierce™ Coomassie Plus (Bradford) Assay Kit (Cat Nr 1856210) according to the manufacturer's instructions in order to load equal amount of proteins. Antibodies were diluted at 1:1000 in PBS - 0.1% Tween - 5% BSA or 5% non-fat dried milk. For stripping, membranes were incubated in a commercial stripping buffer (Cat. Nr ST010; Gene Bio-Application) according to the manufacturer's instructions. Western-blot quantifications were done in FIJI.

RNA interference

For siRNA depletion, 200 000 cells were plated in 6 well plates. After 24 h, cells were treated with the indicated siRNA (30 nM) using RNAimax (Invitrogen, Carlsbad, CA) according to the manufacturer's instruction. Protein depletion was maximal after 72 h of siRNA treatment as shown by immunoblotting analysis with specific antibodies. To deplete CHC, α-adaptin or μ2-adaptin, cells were transfected once as described above and then a second time, 48 hours later, with the same siRNAs. In this case, cells were analyzed 96 hours after the first transfection. The following siRNAs were used: μ2-adaptin, 5'-AAGUGGAUGCCUUUCGGGUCA-3'; Clathrin heavy chain (CHC), 5'GCUGGGAAAACUCUUCAGATT-3'; α-adaptin, 5'-AUGGCGGUGGUGUCGGCUCTT-3'; Epidermal growth factor receptor (EGFR) 5'-GAGGAAAUAUGUACUACGA-3' (EGFR-1) and 5'-GCAAAGUGUGUAACGGAAUAGGUAU-3' (EGFR-2); non-targeting siRNAs (siControl), ON-TARGETplus Non-Targeting SMARTpool siRNAs (Dharmacon D-001810-01). It should be

noted that the AP2 complex is stable only when all of its subunits respect a precise stoichiometric ratio and, consequently, depletion of any of the subunits of AP2 leads to loss of all the components of the complex (Boucrot et al., 2010; Motley et al., 2006).

Immunofluorescence microscopy and fluorescence quantification

For anti-Phosphotyrosine staining (P-Tyr), cells were briefly extracted for 30 s using 0.1% Triton prior to fixation in methanol for 10 min. HeLa cells genome edited to express an endogenous GFP-tagged or mCherry-tagged µ2 subunit were fixed for 2 min in methanol and immunostained. Images were acquired on a Leica Sp8 confocal *with a* Pecon incubation chamber, equipped with 2 Hybrid and 3 PMT detectors, using 405, 488, 561, 633 lasers. The imaging was performed using the ×63 objective (1.4 NA) if not specified otherwise. Fluorescence of selected regions was measured on at least 50 structures of 5 different cells per condition in three independent experiments. Data are expressed as mean ± SD. Colocalization between GFP or mCherry tagged AP2 and Alexa 568 or Alexa 488 immunostained AP2 was measured with the FIJI plugin JACoP (Bolte and Cordelières, 2006).

Spinning disk microscopy of live cells

For CCSs dynamics, cells were imaged at 5 s intervals for the indicated time using a spinning disk microscope (Andor) based on a CSU-W1 Yokogawa head mounted on the lateral port of an inverted IX-83 Olympus microscope equipped with a 60x 1.35NA UPLSAPO objective lens and a laser combiner system, which included 491 and 561 nm 30 mW DPSS lasers (Andor). Images were acquired with a Zyla sCMOS camera (Andor). Alternatively, cells were imaged on a Nikon Ti2 Eclipse (Nikon France SAS, Champigny sur Marne, France) inverted microscope equipped with a 60x NA 1.40 Oil objective WD 0.130, a sCMOS PRIME 95B camera (Photometrics, AZ,

USA) and a dual output laser launch, which included 405, 488, 561 and 642 nm 30 mW lasers. The emission filters characteristics are as follows 452/45nm (Semrock Part# FF01-452/45); 470/24 (Chroma 348716); 525/50nm (Semrock Part# FF03-525/50); 545/40nm (Chroma 346986); 6986); (Semrock Part# FF01-609/54); 708/75nm (Semrock Part# FF01 708/75). Both microscopes were steered by Metamorph 7 software (MDS Analytical Technologies, Sunnyvale, CA, USA).

For CCS dynamics quantification, the lifetime of CCSs was measured using the TrackMate plugin of FIJI (Tinevez et al., 2017). Tracks below 5 seconds of duration (detected on only 1 frame) were discarded. Measured individual lifetimes were pooled into two groups: the "dynamic" group corresponding to structures with a lifetime below the duration of the movie (5 min) and the "static" group with a lifetime of 5 min. Of note, the relative percentage of dynamic versus static structures would be dependent on the duration of the movie because static structures are only counted once while dynamic structures continuously nucleate and disappear during the movie. To circumvent this limitation, all quantifications of CCS dynamics represent the relative number of static or dynamic events detectable at the plasma membrane at a given time point. At least 1000 CCSs from at least 5 cells per conditions and per experiments were tracked in 3-5 independent experiments. Data are expressed as mean ± SD.

Total internal reflection fluorescence microscopy (TIRF) and Fluorescence Recovery After Photobleaching (FRAP)

For total internal reflection fluorescence microscopy (TIRF), HeLa cells transfected with the indicated plasmids were imaged through a 100x 1.49 NA APO TIRF WD 0.13-0.20 oil objective lens on a Nikon Ti2 Eclipse (Nikon France SAS, Champigny sur Marne, France) inverted microscope equipped with a sCMOS PRIME 95B camera (Photometrics, AZ, USA) and a dual

output laser launch, which included 405, 488, 561 and 642 nm 30 mW lasers, and driven by Metamorph 7 software (MDS Analytical Technologies, Sunnyvale, CA, USA). A motorized device (Piezo electrical XYZ stage from Nikon) driven by Metamorph allowed the accurate positioning of the illumination light for evanescent wave excitation.

For TIRF-FRAP experiments, one CCS was manually selected and subjected to 100% laser power (30 mW laser) scan in order to have a bleaching of at least 80% of the fluorescence. One frame was collected before photo-bleaching, and 60 frames were collected after bleaching to analyze fluorescent recovery at the frequency of 1 frame/2 sec. The data were analyzed using the FIJI FRAP Profiler plugin (McMaster University, Canada) to extract recovery curves and calculate the half-time recovery.

Apoptosis assays

3E5 cells were plated on 6 well plates. 24 h later, compression assays were performed. Cells were trypsinized, resuspended in 1ml of medium, washed with ice cold PBS, resuspended in binding buffer (0.1 M Hepes (pH 7.4) 1.4 M NaCl, 25 mM CaCl2) at a density of 1E6 cells/ml. 1E5 cells were then mixed with 5 µl of Annexin-V-Cy5.5 and DAPI (final concentration 1µg/ml) and incubated at RT for 15 minutes. Then, flow cytometry analysis was performed on a BD FACSAria Fusion. Data were analyzed with FlowJo 10.0.7. Cells positive for Annexin V and negative for DAPI were counted as early apoptotic. 3 matched experiments per conditions were performed and data are represented as mean ± SD.

Statistical analyses

Statistical analyses in Fig.1 (panels b, c), Fig.2 (panels f, h), Fig.3 (panel e), Fig.5 (panel f), Supplementary Fig.3 (panel h) were performed using One Way Analysis of Variance (ANOVA).

Statistical analyses in Fig.2 (panels b, j), Fig.3 (panel b), Fig.4 (panel b), Supplementary Fig.1 (panel h), Supplementary Fig.2 (panel b), Supplementary Fig.3 (panel b, d and f) were performed using Kruskal-Wallis One Way analysis of variance on ranks. Statistical analyses in Fig.2 (panel d), Fig.5 (panel b, d), Supplementary Fig.1 (panel g), were performed using two tailed Student's T-test. Statistical analyses in Fig.4 (panel c) was performed using Wilcoxon test. All data are presented as mean of at least three independent experiments ± SD, except otherwise stated. Graphics were prepared with the open-source software Instant Clue (Nolte et al., 2018) and statistical analyses were performed using SigmaPlot or Instant Clue software.

Data availability

The authors declare that all data supporting the findings of this study are available within the article and its supplementary information files or from the corresponding author upon reasonable request.

References:

Alessandri, K., Sarangi, B. R., Gurchenkov, V. V., Sinha, B., Kiessling, T. R., Fetler, L., Rico, F., Scheuring, S., Lamaze, C., Simon, A., et al. (2013). Cellular capsules as a tool for multicellular spheroid production and for investigating the mechanics of tumor progression in vitro. *Proc. Natl. Acad. Sci.* **110**, 14843–14848.

Baschieri, F., Dayot, S., Elkhatib, N., Ly, N., Capmany, A., Schauer, K., Betz, T., Vignjevic, D. M., Poincloux, R. and Montagnac, G. (2018). Frustrated endocytosis controls contractility-independent mechanotransduction at clathrin-coated structures. *Nat. Commun.* **9**,.

Bolte, S. and Cordelières, F. P. (2006). A guided tour into subcellular colocalization analysis in light microscopy. *J. Microsc.* **224**, 213–232.

Bonifacino, J. S. and Traub, L. M. (2003). Signals for Sorting of Transmembrane Proteins to Endosomes and Lysosomes. *Annu. Rev. Biochem.* **72**, 395–447.

Boucrot, E., Saffarian, S., Zhang, R. and Kirchhausen, T. (2010). Roles of AP-2 in Clathrin-Mediated Endocytosis. *PLoS One* **5**, e10597.

Boulant, S., Kural, C., Zeeh, J.-C., Ubelmann, F. and Kirchhausen, T. (2011). Actin dynamics counteract membrane tension during clathrin-mediated endocytosis. *Nat. Cell Biol.* **13**, 1124.

Bucher, D., Mukenhirn, M., Sochacki, K. A., Saharuka, V., Huck, C., Zambarda, C., Taraska, justin, Cavalcanti-Adam, E. A. and Boulant, S. (2018). Focal adhesion-generated cues in extracellular matrix regulate cell migration by local induction of clathrin-coated plaques. *bioRxiv* 493114.

Butcher, D. T., Alliston, T. and Weaver, V. M. (2009). A tense situation: forcing tumour progression. *Nat. Rev. Cancer* **9**, 108–122.

Chen, Y., Yong, J., Martínez-Sánchez, A., Yang, Y., Wu, Y., De Camilli, P., Fernández-Busnadiego, R. and Wu, M. (2019). Dynamic instability of clathrin assembly provides proofreading control for endocytosis. *J. Cell Biol.* jcb.201804136.

Cheng, G., Tse, J., Jain, R. K. and Munn, L. L. (2009). Micro-Environmental Mechanical Stress Controls Tumor Spheroid Size and Morphology by Suppressing Proliferation and Inducing Apoptosis in Cancer Cells. *PLoS One* **4**, e4632.

De Deyne, P. G., O'Neill, A., Resneck, W. G., Dmytrenko, G. M., Pumplin, D. W. and Bloch, R. J. (1998). The vitronectin receptor associates with clathrin-coated membrane

domains via the cytoplasmic domain of its beta5 subunit. *J. Cell Sci.* **111 (Pt 1**, 2729–40.

Eichel, K., Jullié, D. and von Zastrow, M. (2016). β-Arrestin drives MAP kinase signalling from clathrin-coated structures after GPCR dissociation. *Nat. Cell Biol.* **18**, 303–310.

Elkhatib, N., Bresteau, E., Baschieri, F., Rioja, A. L., Van Niel, G., Vassilopoulos, S. and Montagnac, G. (2017). Tubular clathrin/AP-2 lattices pinch collagen fibers to support 3D cell migration. *Science (80-.).* **356**,.

Ferguson, J. P., Huber, S. D., Willy, N. M., Aygün, E., Goker, S., Atabey, T. and Kural, C. (2017). Mechanoregulation of clathrin-mediated endocytosis. *J. Cell Sci.* **130**, 3631–3636.

Fernández-Sánchez, M. E., Barbier, S., Whitehead, J., Béalle, G., Michel, A., Latorre-Ossa, H., Rey, C., Fouassier, L., Claperon, A., Brullé, L., et al. (2015). Mechanical induction of the tumorigenic β-catenin pathway by tumour growth pressure. *Nature* **523**, 92–95.

Gauthier, N. C., Masters, T. A. and Sheetz, M. P. (2012). Mechanical feedback between membrane tension and dynamics. *Trends Cell Biol.* **22**, 527–535.

Heit, B. and Kubes, P. (2003). Measuring Chemotaxis and Chemokinesis: The Under-Agarose Cell Migration Assay. *Sci. Signal.* **2003**, pl5–pl5.

Kalli, M. and Stylianopoulos, T. (2018). Defining the Role of Solid Stress and Matrix Stiffness in Cancer Cell Proliferation and Metastasis. *Front. Oncol.* **8**, 55.

Lamaze, C. and Schmid, S. L. (1995). Recruitment of epidermal growth factor receptors into coated pits requires their activated tyrosine kinase. *J. Cell Biol.* **129**, 47–54.

McMahon, H. T. and Boucrot, E. (2011). Molecular mechanism and physiological functions of clathrin-mediated endocytosis. *Nat. Rev. Mol. Cell Biol.* **12**, 517–533.

Motley, A. M., Berg, N., Taylor, M. J., Sahlender, D. A., Hirst, J., Owen, D. J. and Robinson, M. S. (2006). Functional analysis of AP-2 α and μ2 subunits. *Mol. Biol. Cell* **17**,

5298–5308.

Nia, H. T., Liu, H., Seano, G., Datta, M., Jones, D., Rahbari, N., Incio, J., Chauhan, V. P., Jung, K., Martin, J. D., et al. (2017). Solid stress and elastic energy as measures of tumour mechanopathology. *Nat. Biomed. Eng.* **1**, 0004.

Nolte, H., MacVicar, T. D., Tellkamp, F. and Krüger, M. (2018). Instant Clue: A Software Suite for Interactive Data Visualization and Analysis. *Sci. Rep.* **8**, 1–8.

Petrelli, A., Gilestro, G. F., Lanzardo, S., Comoglio, P. M., Migone, N. and Giordano, S. (2002). The endophilin–CIN85–Cbl complex mediates ligand-dependent downregulation of c-Met. *Nature* **416**, 187–190.

Rakesh, K., Yoo, B., Kim, I.-M., Salazar, N., Kim, K.-S. and Rockman, H. A. (2010). beta-Arrestin-biased agonism of the angiotensin receptor induced by mechanical stress. *Sci. Signal.* **3**, ra46.

Rappoport, J. Z. and Simon, S. M. (2009). Endocytic trafficking of activated EGFR is AP-2 dependent and occurs through preformed clathrin spots. *J. Cell Sci.* **122**, 1301–1305.

Raucher, D. and Sheetz, M. P. (1999). Membrane expansion increases endocytosis rate during mitosis. *J. Cell Biol.* **144**, 497–506.

Saleem, M., Morlot, S., Hohendahl, A., Manzi, J., Lenz, M. and Roux, A. (2015). A balance between membrane elasticity and polymerization energy sets the shape of spherical clathrin coats. *Nat. Commun.* **6**, 6249.

Shojaei, F., Lee, J. H., Simmons, B. H., Wong, A., Esparza, C. O., Plumlee, P. A., Feng, J., Stewart, A. E., Hu-Lowe, D. D. and Christensen, J. G. (2010). HGF/c-Met Acts as an Alternative Angiogenic Pathway in Sunitinib-Resistant Tumors. *Cancer Res.* **70**, 10090–10100.

Sigismund, S., Argenzio, E., Tosoni, D., Cavallaro, E., Polo, S. and Di Fiore, P. P. (2008). Clathrin-Mediated Internalization Is Essential for Sustained EGFR Signaling but Dispensable for Degradation. *Dev. Cell* **15**, 209–219.

Straussman, R., Morikawa, T., Shee, K., Barzily-Rokni, M., Qian, Z. R., Du, J., Davis, A., Mongare, M. M., Gould, J., Frederick, D. T., et al. (2012). Tumour micro-environment elicits innate resistance to RAF inhibitors through HGF secretion. *Nature* **487**, 500–504.

Tinevez, J.-Y., Perry, N., Schindelin, J., Hoopes, G. M., Reynolds, G. D., Laplantine, E., Bednarek, S. Y., Shorte, S. L. and Eliceiri, K. W. (2017). TrackMate: An open and extensible platform for single-particle tracking. *Methods* **115**, 80–90.

Tschumperlin, D. J., Shively, J. D., Swartz, M. A., Silverman, E. S., Haley, K. J., Raab, G. and Drazen, J. M. (2002). Bronchial epithelial compression regulates MAP kinase signaling and HB-EGF-like growth factor expression. *Am. J. Physiol. Cell. Mol. Physiol.* **282**, L904–L911.

Tschumperlin, D. J., Dai, G., Maly, I. V., Kikuchi, T., Laiho, L. H., McVittie, A. K., Haley, K. J., Lilly, C. M., So, P. T. C., Lauffenburger, D. A., et al. (2004). Mechanotransduction through growth-factor shedding into the extracellular space. *Nature* **429**, 83–86.

Vieira, A. V., Lamaze, C. and Schmid, S. L. (1996). Control of EGF Receptor Signaling by Clathrin-Mediated Endocytosis. *Science (80-.).* **274**, 2086–2089.

Wang, Y., Pennock, S., Chen, X. and Wang, Z. (2002). Endosomal signaling of epidermal growth factor receptor stimulates signal transduction pathways leading to cell survival. *Mol. Cell. Biol.* **22**, 7279–90.

Wang, Q., Villeneuve, G. and Wang, Z. (2005). Control of epidermal growth factor receptor endocytosis by receptor dimerization, rather than receptor kinase activation. *EMBO Rep.* **6**,

942–948.

Zhang, X., Nie, D. and Chakrabarty, S. (2010). Growth factors in tumor microenvironment. *Front. Biosci. (Landmark Ed.* **15**, 151–65.

Acknowledgment:

We thank the imaging facilities of Gustave Roussy for help with image acquisition. Core funding for this work was provided by the Gustave Roussy Institute and the Inserm and additional support was provided by grants from ATIP/Avenir Program, la Fondation ARC pour la Recherche sur le cancer, Le Groupement des Entreprises Françaises dans la LUtte contre le Cancer (GEFLUC) and from the Agence Nationale de la Recherche (ANR-15-CE15-0005-03) to GM. This project was supported by grant "Taxe d'apprentissage Gustave Roussy - 2017 - DLD". FB acknowledges support by the 2019 metastasis award from the Beug Foundation.

F.B designed and performed experiments, analysed results and wrote the manuscript. N.E, D.L.D. and S.T. performed experiments. G.M supervised the study, designed experiments and wrote the manuscript.

The authors declare no competing interests. Correspondence and requests for materials should be addressed to guillaume.montagnac@gustaveroussy.fr or to francesco.baschieri@gustaveroussy.fr

Figure legends:

Figure 1. **Cell compression reduces CCSs dynamics a**, Kymographs showing CCS dynamics in genome-edited HeLa cells expressing endogenous mCherry-tagged μ2-adaptin compressed or not under an agarose plug and treated or not with Cilengitide, as indicated, and imaged by spinning disk microscopy every 5s for 5 min. **b**, **c**, Quantification of the dynamics of CCSs observed as in a (* P<0.05; ** P<0.001, as compared to control condition, One Way Analysis of Variance – ANOVA. N=3). **d**, Gallery depicting fluorescence recovery of a single CCS (arrows) after photobleaching in control (upper panels) or compressed (lower panels) cells. Time before or after photobleaching is indicated in seconds. Scale bar: 1μm. **e**, Quantification of fluorescence recovery as in d in control or compressed cells as indicated. All results are expressed as mean ± SD.

Figure 2. **CCSs are required for EGFR-dependent signaling. a**, Western-blot analysis of phospho-ERK (P-ERK) levels in HeLa cells uncompressed (control) or compressed for different time periods as indicated (representative image of three independent experiments). Total-ERK was used as loading control. **b,** Densitometry analysis of bands obtained in Western-blots as in a. Results are expressed as mean ratio of P-ERK/total ERK ± SD from three independent experiments. (** P<0.005, *** P<0.001, Kruskal-Wallis One Way analysis of variance on ranks). **c,** Western-blot analysis of phospho-ERK (P-ERK) levels in the indicated cell lines compressed or not for 30 min (representative image of three independent experiments). Total-ERK was used as loading control. **d,** Densitometry analysis of bands obtained in Western-blots as in c. Results are expressed as mean ratio of P-ERK/total ERK ± SD from 3 independent experiments (* *P*<0.05; *** P<0.001, two-tailed paired t-test). **e**, Western-blot analysis of phospho-ERK (P-ERK) levels in HeLa cells compressed or not for 30 min and treated or not with EGFR specific siRNAs as

indicated (representative image of four independent experiments). Total-ERK was used as loading control. **f**, Densitometry analysis of bands obtained in Western-blots as in e. Results are expressed as mean ratio of P-ERK/total ERK ± SD from four independent experiments (* $P<0.05$, One Way Analysis of Variance – ANOVA). **g**, Western-blot analysis of phospho-ERK (P-ERK) levels in HeLa cells compressed or not for 30 min and treated or not with Gefitinib for 1 h prior to compression (representative image of three independent experiments). Total-ERK was used as loading control. **h**, Densitometry analysis of bands obtained in Western-blots as in g. Results are expressed as mean ratio of P-ERK/total ERK ± SD from three independent experiments (* $P<0.05$, One Way Analysis of Variance – ANOVA). **i**, Western-blot analysis of phospho-ERK (P-ERK) levels in HeLa cells compressed or not for 30 min and treated or not with AP-2 subunits- or CHC-specific siRNAs as indicated (representative image of five independent experiments). Total-ERK was used as loading control. **j**, Densitometry analysis of bands obtained in Western-blots as in i. Results are expressed as mean ratio of P-ERK/total ERK ± SD from five independent experiments (* $P<0.05$, ** $P<0.005$ Kruskal-Wallis One Way analysis of variance on ranks).

Figure 3. **EGFR is recruited at CCSs under compression. a**, Genome-edited HeLa cells expressing endogenous mCherry-tagged μ2-adaptin were transfected with a plasmid encoding eGFP-tagged EGFR, seeded on glass, compressed under an agarose plug and imaged by TIRF microscopy every 15s for 30 min. Time after compression is indicated. Higher magnifications of boxed regions are shown. Arrows point to EGFR positive CCSs. Scale bar: 8 μm. **b**, Quantification of eGFP-EGFR enrichment at CCSs at the indicated time points after compression in control cells or in cells treated with Batimastat or with Gefitinib, as indicated (** $P<0.001$ compared to Batimastat, Kruskal-Wallis One Way analysis of variance on ranks. N=3; 20 structures per

experiment were analysed). **c**, Genome-edited HeLa cells expressing endogenous mCherry-tagged μ2-adaptin were transfected with a plasmid encoding eGFP-tagged EGFR and seeded on glass. 24 h later, cells were serum starved for 2 h, treated with 10 μM Gefitinib for 1 h, then compressed under an agarose plug and imaged by TIRF microscopy every 15s for 30 min. Time after compression is indicated. Scale bar: 1 μm. **d**, Genome-edited HeLa cells expressing endogenous mCherry-tagged μ2-adaptin were transfected with a plasmid encoding eGFP-tagged EGFR and seeded on glass. 24 h later, cells were serum starved for 2 h, treated with Batimastat for 1 h, then compressed under an agarose plug and imaged by TIRF microscopy every 15s for 30 min. Time after compression is indicated. Scale bar: 1 μm. **e**, Western-blot analysis of phospho-ERK (P-ERK) levels in HeLa cells serum starved for 2 hours, then treated with 10 μM Batimastat for 1h, and subjected or not to compression, as indicated (representative image of four independent experiments). Total-ERK1/2 was used as a loading control. **f,** Densitometry analysis of bands obtained in Western-blots as in e. Results are expressed as mean ratio of P-ERK/total ERK ± SD from three independent experiments (* $P<0.05$, One Way Analysis of Variance – ANOVA).

Figure 4. **Receptors are sorted differently in CCSs under compression. a**, Genome-edited HeLa cells expressing endogenous eGFP-tagged μ2-adaptin were transfected with a plasmid encoding mCherry-tagged TfR and were imaged by TIRF microscopy before (upper panel) or 5 min after (lower panel) compression. Arrows point to TfR positive CCSs. Arrowheads point to TfR-positive, AP-2-negative structures most likely corresponding to endosomes. Scale bar: 2 μm. **b**, Quantification of mCherry-TfR enrichment at CCSs before or 5 min after compression in cells treated as in a (* $P<0.05$, Kruskal-Wallis One Way analysis of variance on ranks. 30 structures per experiment were analysed in three independent experiments). **c,** TfR average intensity at the

ventral plasma membrane of HeLa cells as in a was measured before and after compression (** P<0.001, Wilcoxon test. 10 cells per experiment were analysed in three independent experiments). **d, e**, Genome-edited HeLa cells expressing endogenous mCherry-tagged μ2-adaptin were transfected with plasmids encoding YFP-tagged AT1R (d) or GFP-tagged HGFR (e), as indicated, seeded on glass, compressed under an agarose plug and imaged by TIRF microscopy every 10s for 30 min. Time after compression is indicated. Scale bars: 1.5 μm.

Figure 5. **CCSs under compression can serve as signaling platform for different receptors.** **a**, Genome-edited HeLa cells expressing endogenous mCherry-tagged μ2-adaptin were transfected with a plasmid encoding eGFP-tagged HGFR. Cells were seeded on glass and 100 ng/ml HGF was added in the culture medium 1h before cells were compressed under an agarose plug and imaged by TIRF microscopy every 10s for 30 min. Time after compression is indicated. Arrows point to HGFR positive CCSs. Scale bar: 2 μm. **b**, Quantification of eGFP-HGFR enrichment at CCSs before or 5 min after compression in control cells treated as in a (** P<0.001, two tailed paired Student's T-test; at least 20 structures per experiment in three independent experiments were analysed). **c**, Genome-edited HeLa cells expressing endogenous mCherry-tagged μ2-adaptin were transfected with a plasmid encoding YFP-tagged AT1R. Cells were seeded on glass and 1 pM Angiotensin II was added in the culture medium 5h before cells were compressed under an agarose plug and imaged by TIRF microscopy every 10s for 30 min. Time after compression is indicated. Arrows point to AT1R positive CCSs. Scale bar: 2.5 μm. **d,** Quantification of YFP-AT1R enrichment at CCSs before or 5 min after compression in control cells treated as in c (** P<0.001, two tailed paired Student's T-test. 50 structures per experiment were analysed in 3 independent experiments). **e**, Western-blot analysis of phospho-ERK (P-ERK) levels in HeLa cells that were

incubated in the presence of HGF for 1h before to be compressed or not and treated or not with Gefitinib, as indicated (representative image of three independent experiments). Total ERK was used as a loading control. **f,** Densitometry analysis of bands obtained in Western-blots as in f. Results are expressed as mean ratio of P-ERK/total ERK ± SD from three independent experiments (* $P<0.05$, One Way Analysis of Variance – ANOVA, Student-Newman-Keuls).

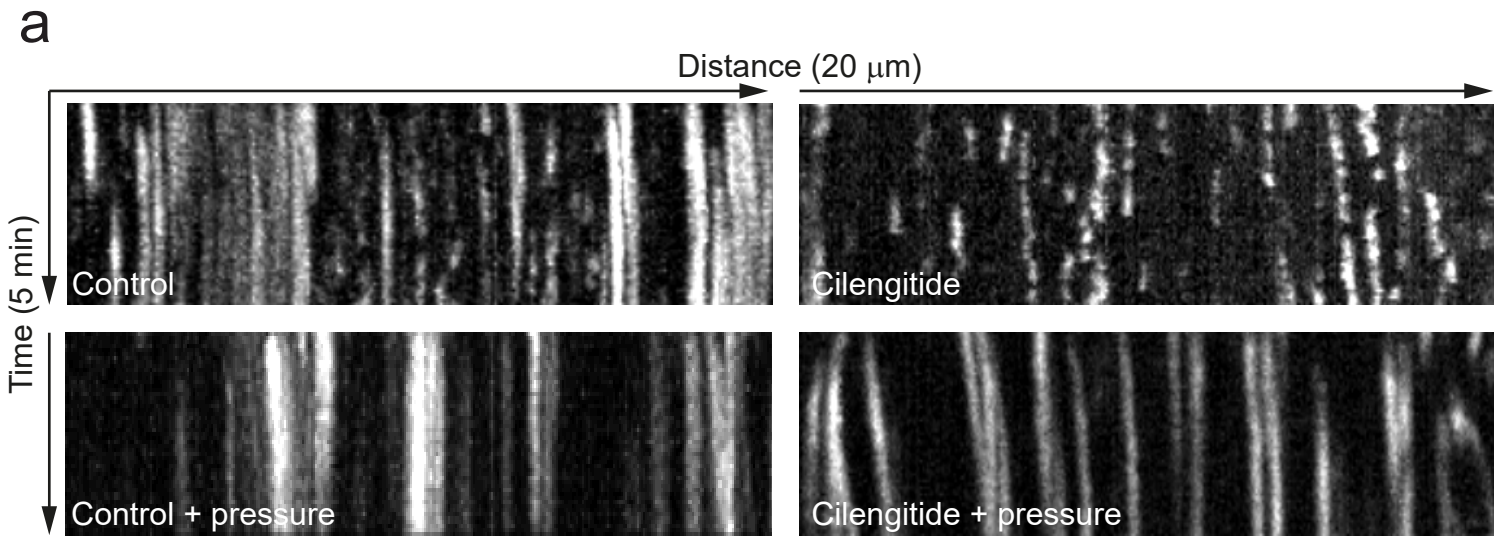
a
Distance (20 μm)
Time (5 min)
Control
Cilengitide
Control + pressure
Cilengitide + pressure

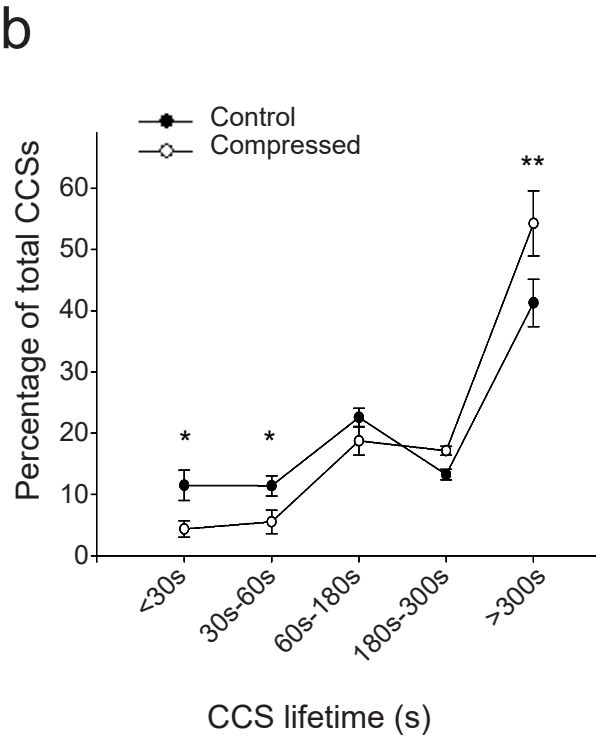
b
Control
Compressed
Percentage of total CCSs
0
10
20
30
40
50
60
*
*
**
<30s
30s-60s
60s-180s
180s-300s
>300s
CCS lifetime (s)

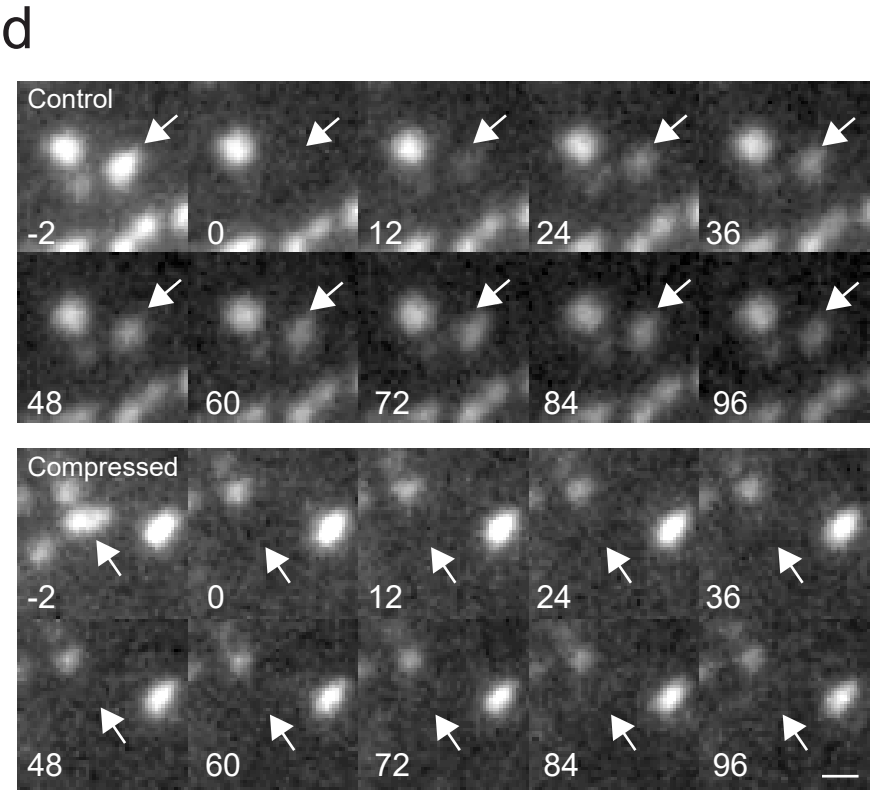
d
Control
-2
0
12
24
36
48
60
72
84
96
Compressed
-2
0
12
24
36
48
60
72
84
96

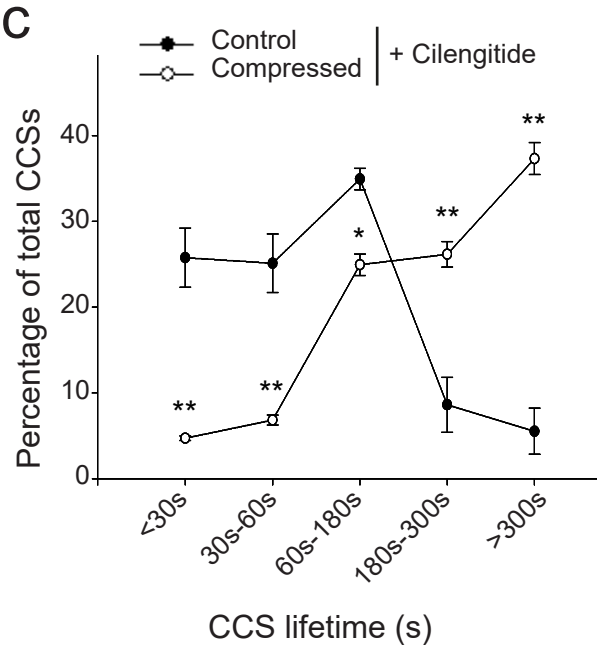
c
Control
Compressed
+ Cilengitide
Percentage of total CCSs
0
10
20
30
40
**
**
*
**
**
**
<30s
30s-60s
60s-180s
180s-300s
>300s
CCS lifetime (s)

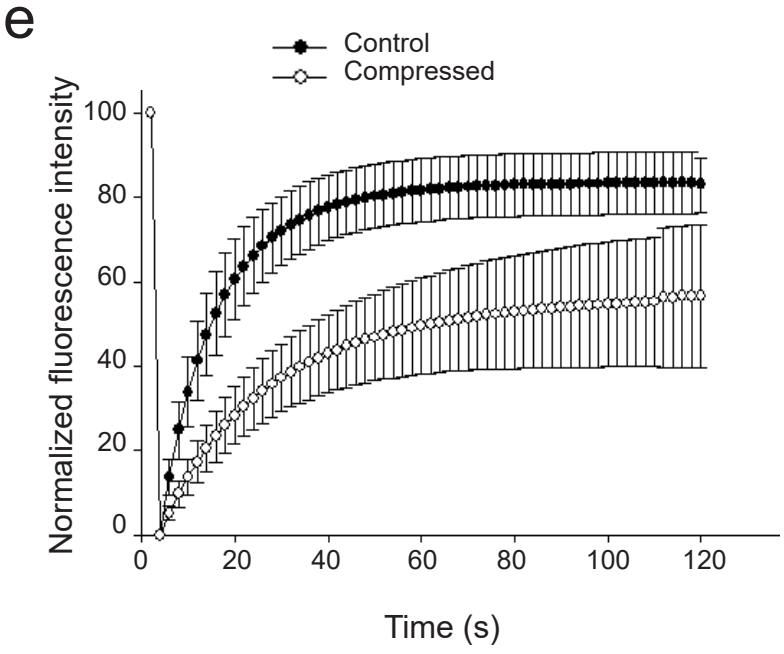
e
Control
Compressed
Normalized fluorescence intensity
0
20
40
60
80
100
0
20
40
60
80
100
120
Time (s)

Figure 1

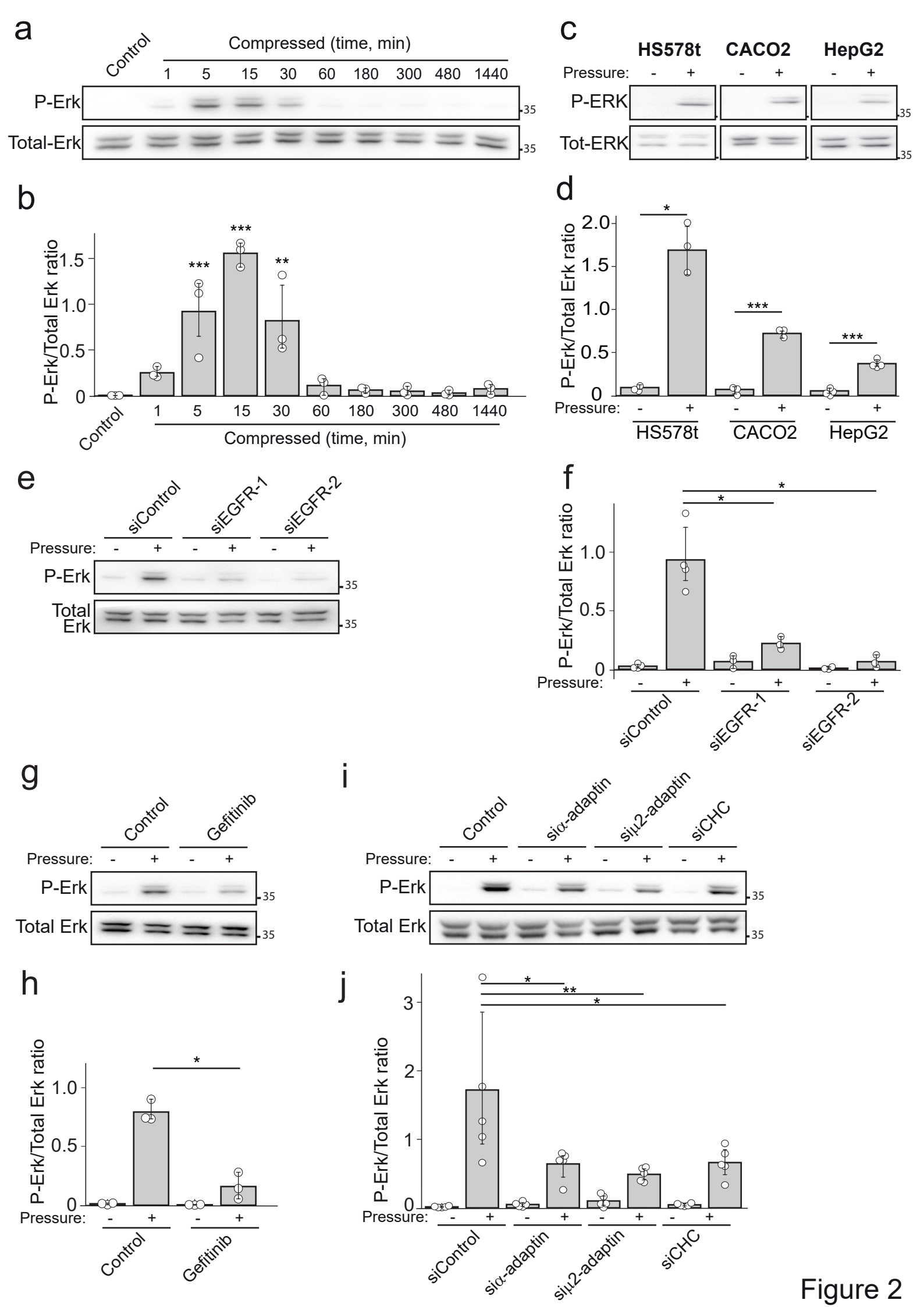
a
Control
Compressed (time, min)
1 5 15 30 60 180 300 480 1440
P-Erk
Total-Erk
35
b
P-Erk/Total Erk ratio
0 0.5 1.0 1.5
***
***
**
Control
1 5 15 30 60 180 300 480 1440
Compressed (time, min)
c
HS578t CACO2 HepG2
Pressure: - + - + - +
P-ERK
Tot-ERK
35
d
P-Erk/Total Erk ratio
0 0.5 1.0 1.5 2.0
*
***
***
Pressure: - + - + - +
HS578t CACO2 HepG2
e
siControl siEGFR-1 siEGFR-2
Pressure: - + - + - +
P-Erk
Total Erk
35
f
P-Erk/Total Erk ratio
0 0.5 1.0
*
*
Pressure: - + - + - +
siControl siEGFR-1 siEGFR-2
g
Control Gefitinib
Pressure: - + - +
P-Erk
Total Erk
35
i
Control siα-adaptin siμ2-adaptin siCHC
Pressure: - + - + - + - +
P-Erk
Total Erk
35
h
P-Erk/Total Erk ratio
0 0.5 1.0
*
Pressure: - + - +
Control Gefitinib
j
P-Erk/Total Erk ratio
0 1 2 3
*
**
*
Pressure: - + - + - + - +
siControl siα-adaptin siμ2-adaptin siCHC

Figure 2

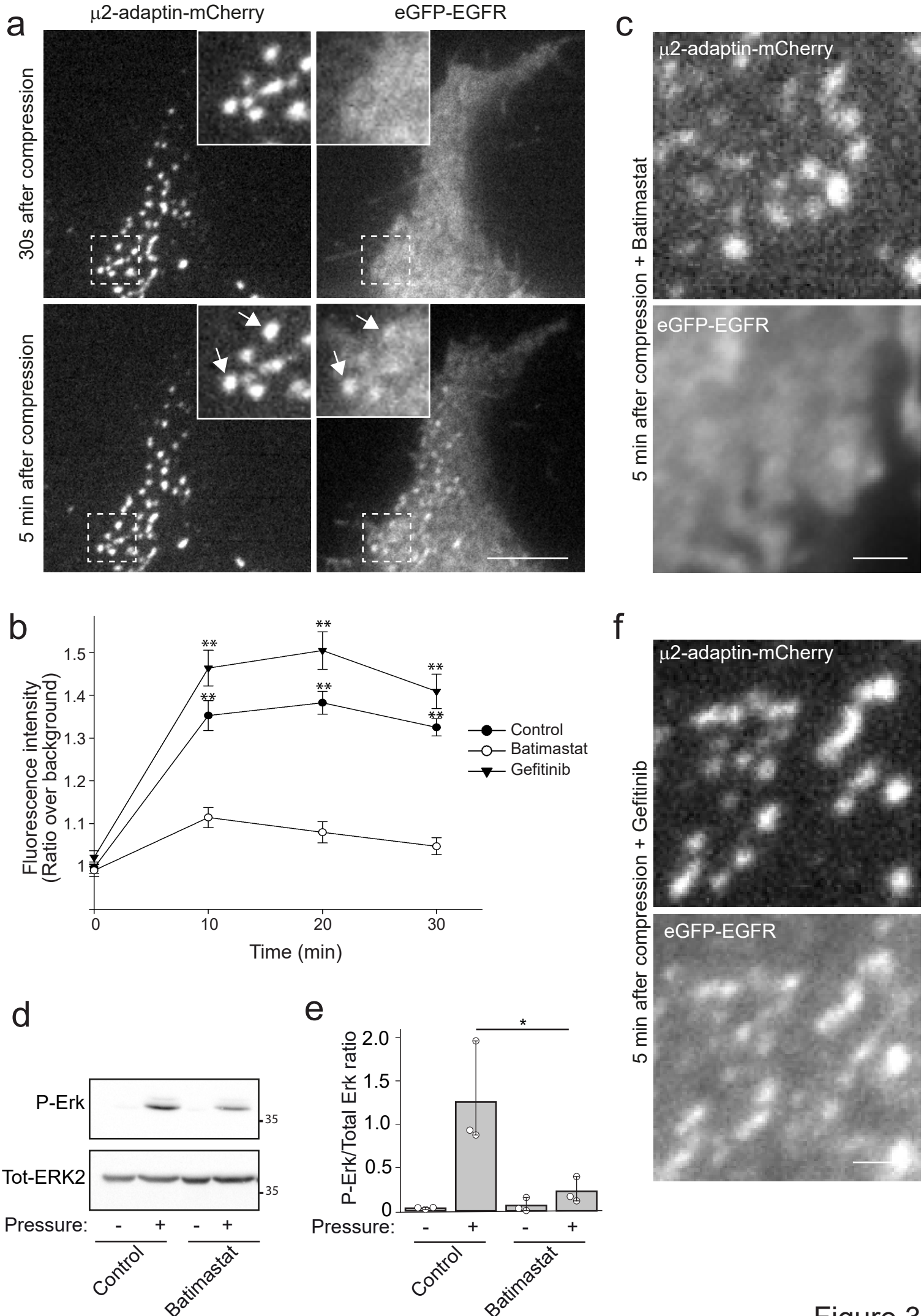
a
μ2-adaptin-mCherry
eGFP-EGFR
30s after compression
5 min after compression
c
μ2-adaptin-mCherry
eGFP-EGFR
5 min after compression + Batimastat
b
Fluorescence intensity
(Ratio over background)
1.5
1.4
1.3
1.2
1.1
1
0
10
20
30
Time (min)
**
Control
Batimastat
Gefitinib
f
μ2-adaptin-mCherry
eGFP-EGFR
5 min after compression + Gefitinib
d
P-Erk
Tot-ERK2
35
35
Pressure: - + - +
Control
Batimastat
e
P-Erk/Total Erk ratio
2.0
1.5
1.0
0.5
0
*
Pressure: - + - +
Control
Batimastat

Figure 3

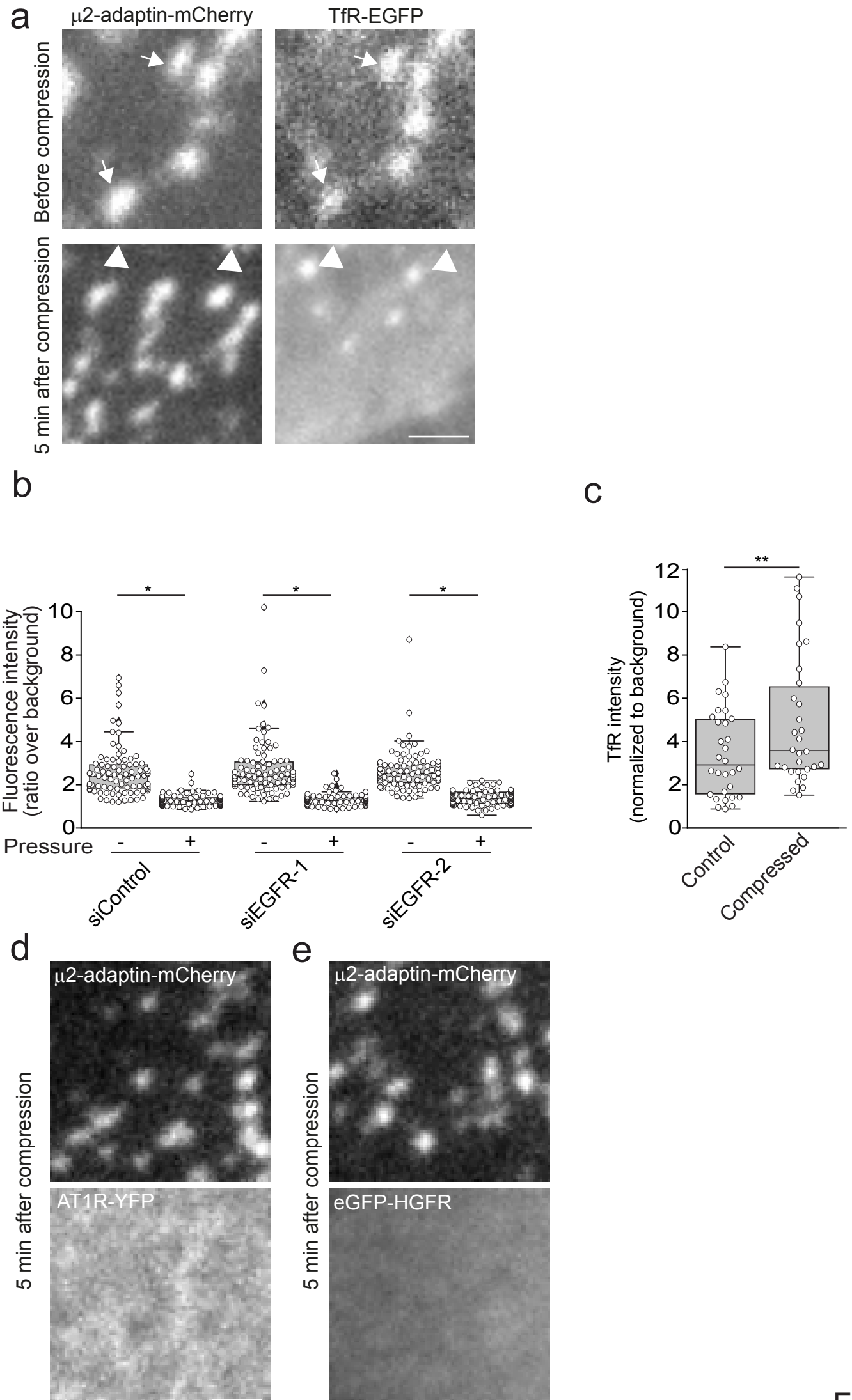
a
μ2-adaptin-mCherry
TfR-EGFP
Before compression
5 min after compression
b
Fluorescence intensity
(ratio over background)
Pressure
siControl
siEGFR-1
siEGFR-2
c
TfR intensity
(normalized to background)
Control
Compressed
d
μ2-adaptin-mCherry
AT1R-YFP
5 min after compression
e
μ2-adaptin-mCherry
eGFP-HGFR
5 min after compression

Figure 4

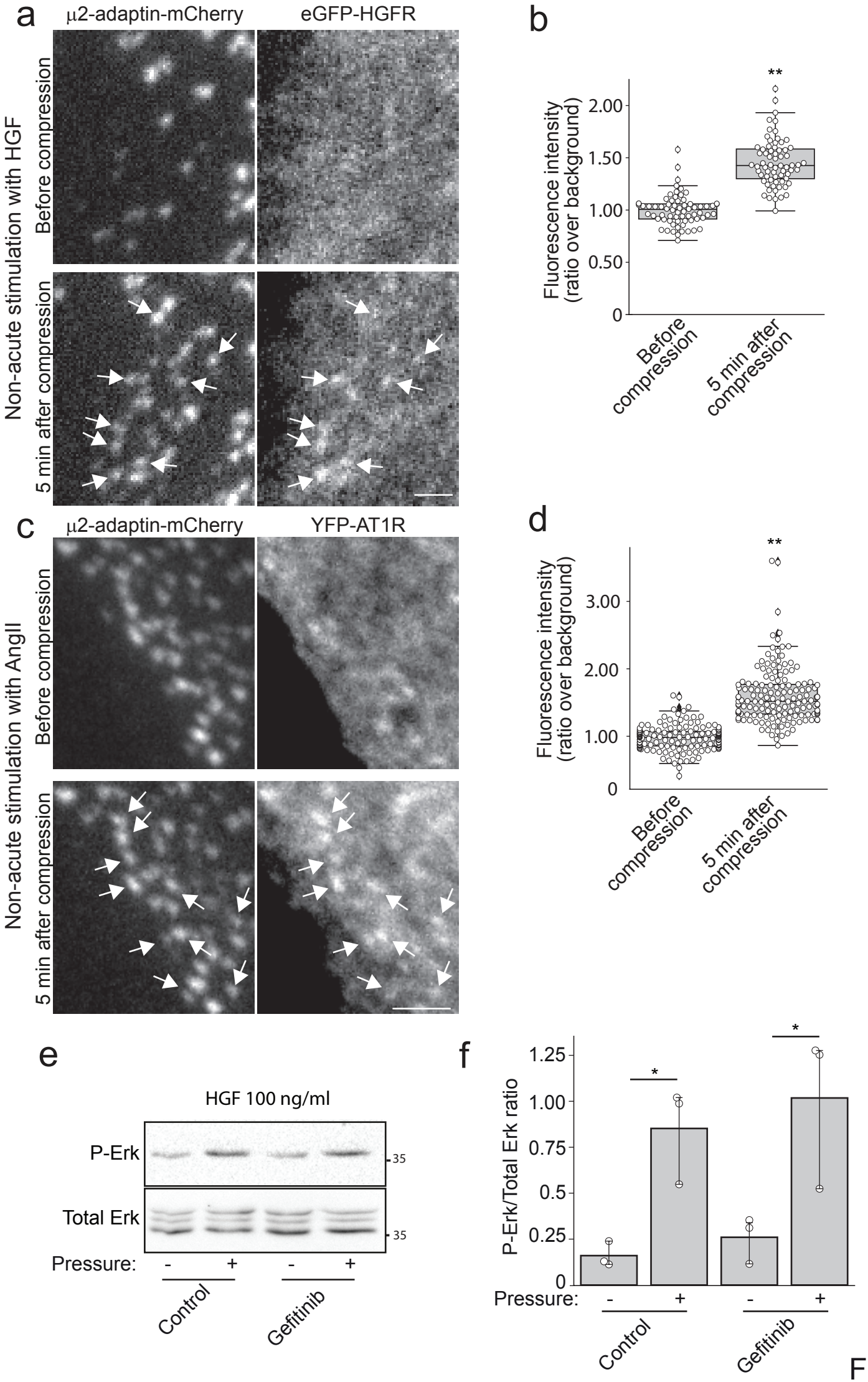
a
μ2-adaptin-mCherry
eGFP-HGFR
Non-acute stimulation with HGF
Before compression
5 min after compression
b
Fluorescence intensity (ratio over background)
2.00
1.50
1.00
0.50
0
**
Before compression
5 min after compression
c
μ2-adaptin-mCherry
YFP-AT1R
Non-acute stimulation with AngII
Before compression
5 min after compression
d
Fluorescence intensity (ratio over background)
3.00
2.00
1.00
0
**
Before compression
5 min after compression
e
HGF 100 ng/ml
P-Erk
Total Erk
35
35
Pressure: - + - +
Control
Gefitinib
f
P-Erk/Total Erk ratio
1.25
1.00
0.75
0.5
0.25
0
*
*
Pressure: - + - +
Control
Gefitinib

Figure 5

SUPPLEMENTARY DATA

Supplementary figures and supplementary figure legends.

Supplementary Videos

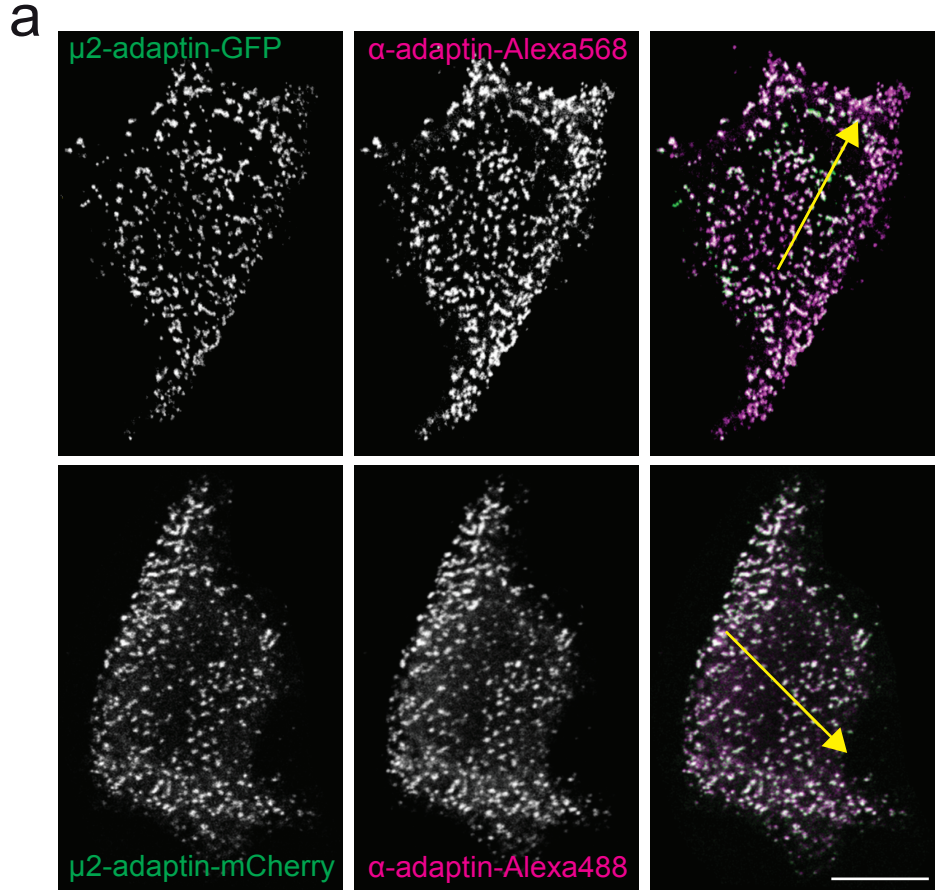
a
μ2-adaptin-GFP
α-adaptin-Alexa568
μ2-adaptin-mCherry
α-adaptin-Alexa488

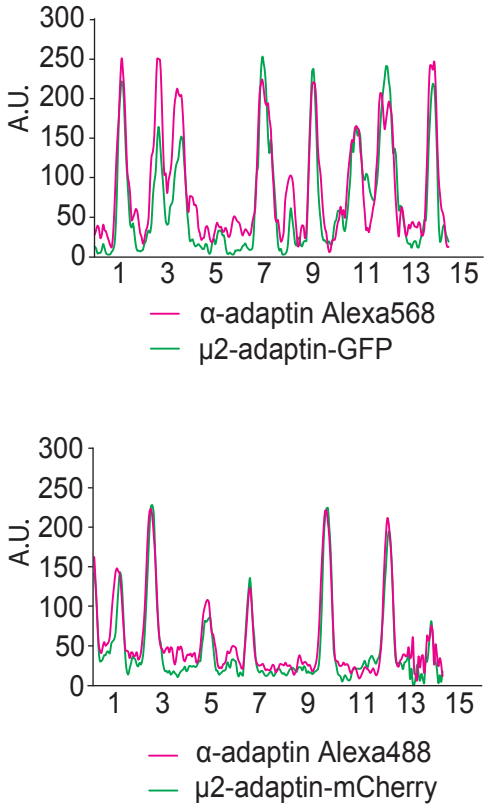
b
A.U.
300
250
200
150
100
50
0
1 3 5 7 9 11 13 15
α-adaptin Alexa568
μ2-adaptin-GFP
A.U.
300
250
200
150
100
50
0
1 3 5 7 9 11 13 15
α-adaptin Alexa488
μ2-adaptin-mCherry

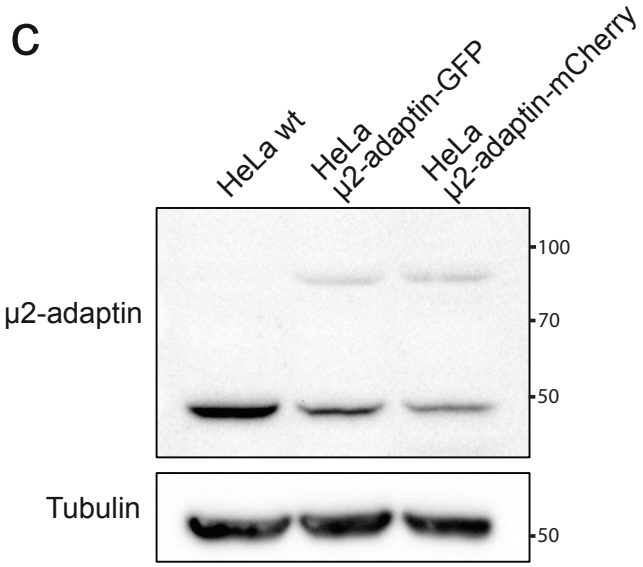
c
HeLa wt
HeLa μ2-adaptin-GFP
HeLa μ2-adaptin-mCherry
μ2-adaptin
100
70
50
Tubulin
50

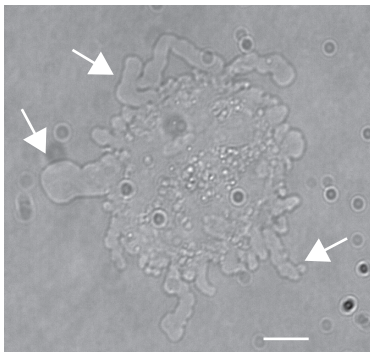
e

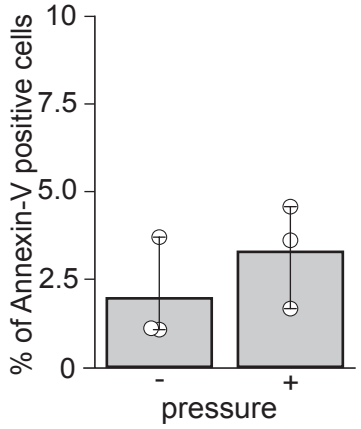
g
% of Annexin-V positive cells
10
7.5
5.0
2.5
0
-
+
pressure

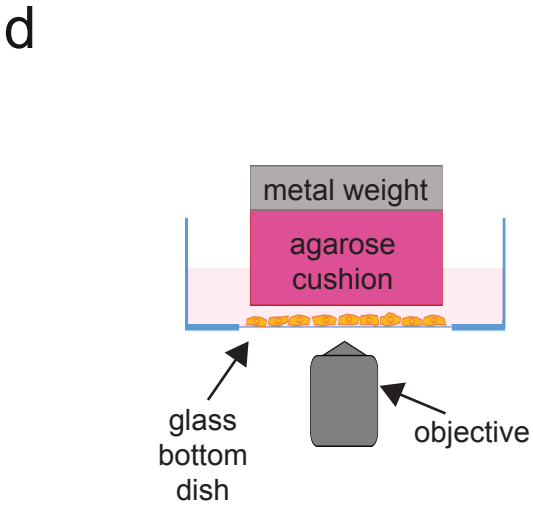
d
metal weight
agarose cushion
glass bottom dish
objective

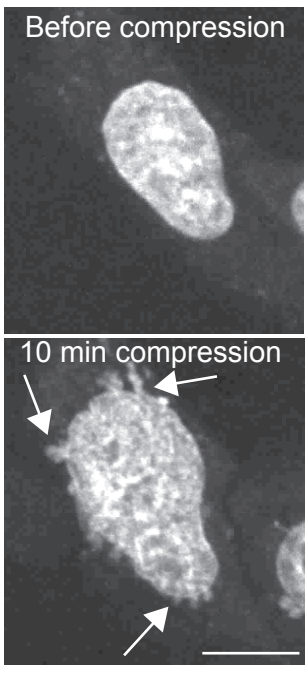
f
Before compression
10 min compression

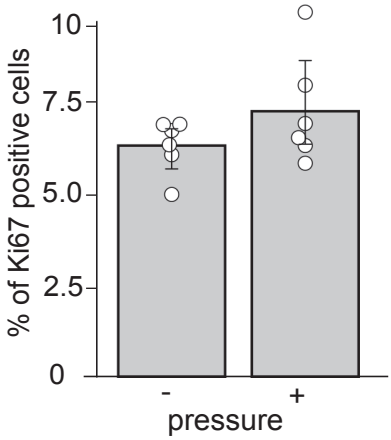
h
% of Ki67 positive cells
10
7.5
5.0
2.5
0
-
+
pressure

Figure S1

Figure S1. **Validation of the cell compression strategy**. **a**, HeLa cells genome-edited to express a fluorescently-tagged version of µ2-adaptin, a subunit of the clathrin adaptor AP-2, were immunostained using antibodies against α-adaptin, another subunit of the AP-2 complex. Scale bar: 10 µm. **b**, Intensity plot corresponding to the regions marked by yellow arrows in images in a. **c**, Western-blot analysis of µ2-adaptin levels in HeLa cells wt or genome-edited to express a fluorescently-tagged version of µ2-adaptin. Tubulin was used as loading control. **d**,schematic of our cell compression imaging set-up. **e**, Wide-field image of one HeLa cell compressed under and agarose plug. Arrows points to blebs at the plasma membrane. Scale bar: 5µm. **f**, HeLa cells treated with Sir-DNA were imaged by spinning disk microscopy before or after compression under an agarose plug, as indicated. Arrows point to nuclear blebs. Scale bar: 10µm. **g**, HeLa cells were subjected or not to compressive stress for 30 min. Cells were then recovered and stained for Annexin V and DAPI according to the manufacturer's instructions. Cells positive for Annexin V and negative for DAPI were counted in three independent experiments. Results are expressed as mean ± SD (two tailed paired Student's T-test). **h**, HeLa cells plated on glass coverslips at 80% confluency were subjected or not to compressive stress. The stress was then removed and the medium changed to eliminate cell debris. 48 h later, cells were fixed and immunostained for Ki-67 and imaged at 20x. The number of Ki-67 positive cells was counted in each condition. Results are expressed as mean ± SD (Kruskal-Wallis One Way analysis of variance on ranks. Three independent experiments were performed, counting cells in 2 random fields, corresponding to approximately 600 cells per condition per experiment).

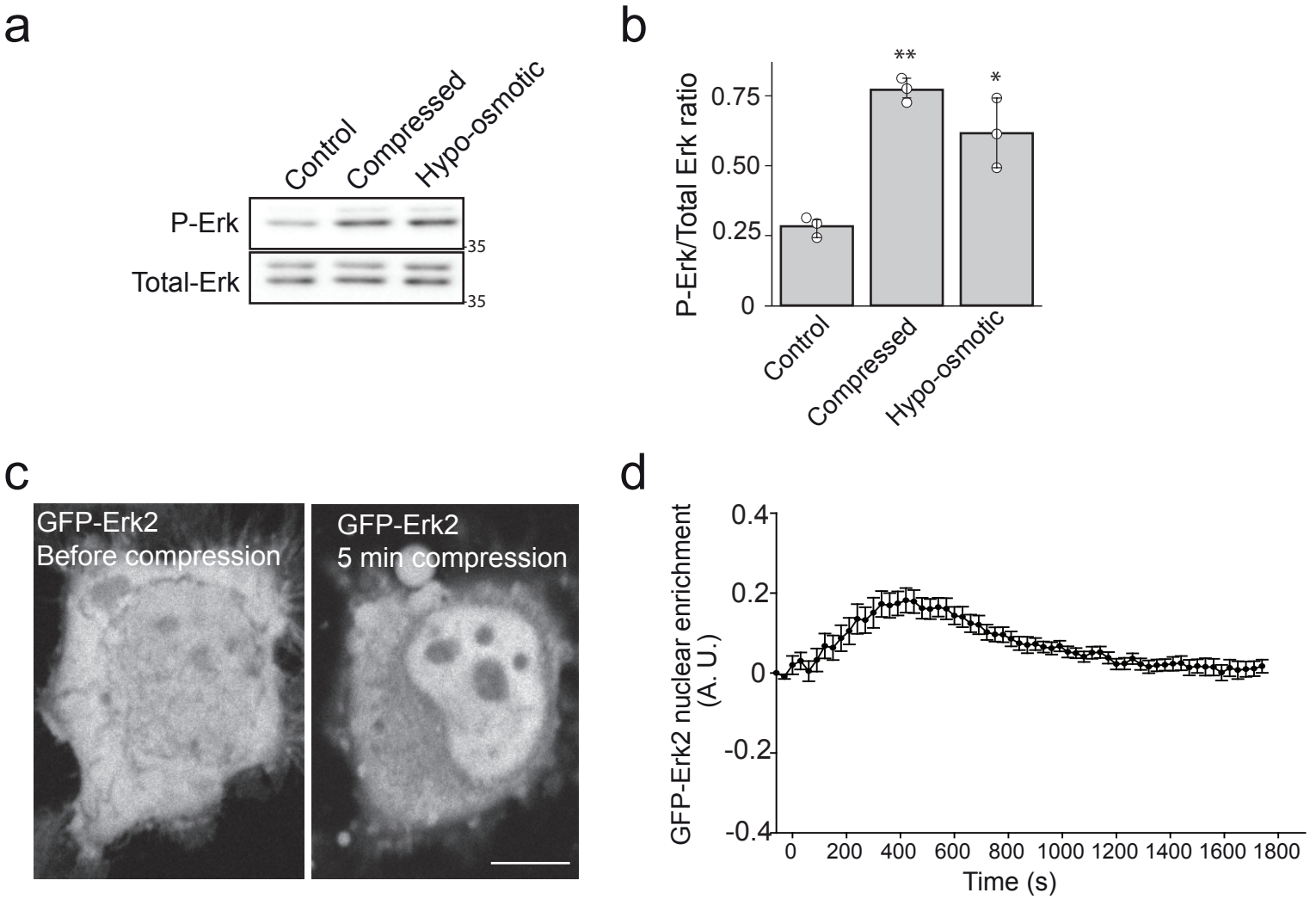
a
Control
Compressed
Hypo-osmotic
P-Erk
Total-Erk
35
35
b
P-Erk/Total Erk ratio
0.75
0.50
0.25
0
**
*
Control
Compressed
Hypo-osmotic
c
GFP-Erk2
Before compression
GFP-Erk2
5 min compression
d
GFP-Erk2 nuclear enrichment
(A. U.)
0.4
0.2
0
-0.2
-0.4
0
200
400
600
800
1000
1200
1400
1600
1800
Time (s)

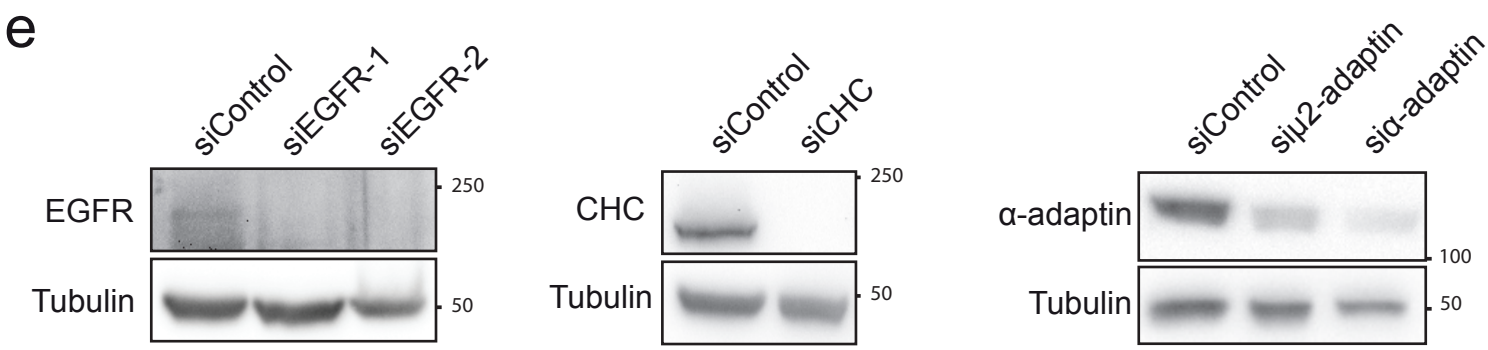
e
siControl
siEGFR-1
siEGFR-2
EGFR
Tubulin
250
50
siControl
siCHC
CHC
Tubulin
250
50
siControl
siμ2-adaptin
siα-adaptin
α-adaptin
Tubulin
100
50

Figure S2

Figure S2. **Analysis on membrane tension and ERK. a**, Western-blot analysis of phospho-ERK (P-ERK) levels in HeLa cells uncompressed (control), compressed, or subjected to hypo-osmotic shock (90% water) for 30 min (representative image of three independent experiments). Total-ERK was used as loading control. **b**, Densitometry analysis of bands obtained in Western-blots as in a. Results are expressed as mean ratio of P-ERK/total ERK ± SD from three independent experiments. (* $P<0.005$, ** $P<0.001$, Kruskal-Wallis One Way analysis of variance on ranks). **c**, HeLa cells transfected with a plasmid encoding eGFP-tagged ERK2 were imaged by spinning disk microscopy before (left panel) or after (right panel) being compressed under an agarose plug. Scale bar: 10μm. **d**, Quantification of eGFP-ERK2 enrichment in the nucleus at the indicated time points after compression. 22 cells from 3 independent experiments were quantified. Results are expressed as mean ± SE.**e,** HeLa cells were transfected with the indicated siRNAs. 72 h after transfection, cells were lysed and subjected to Western-blot analysis using the indicated antibodies. Tubulin was used as a loading control.

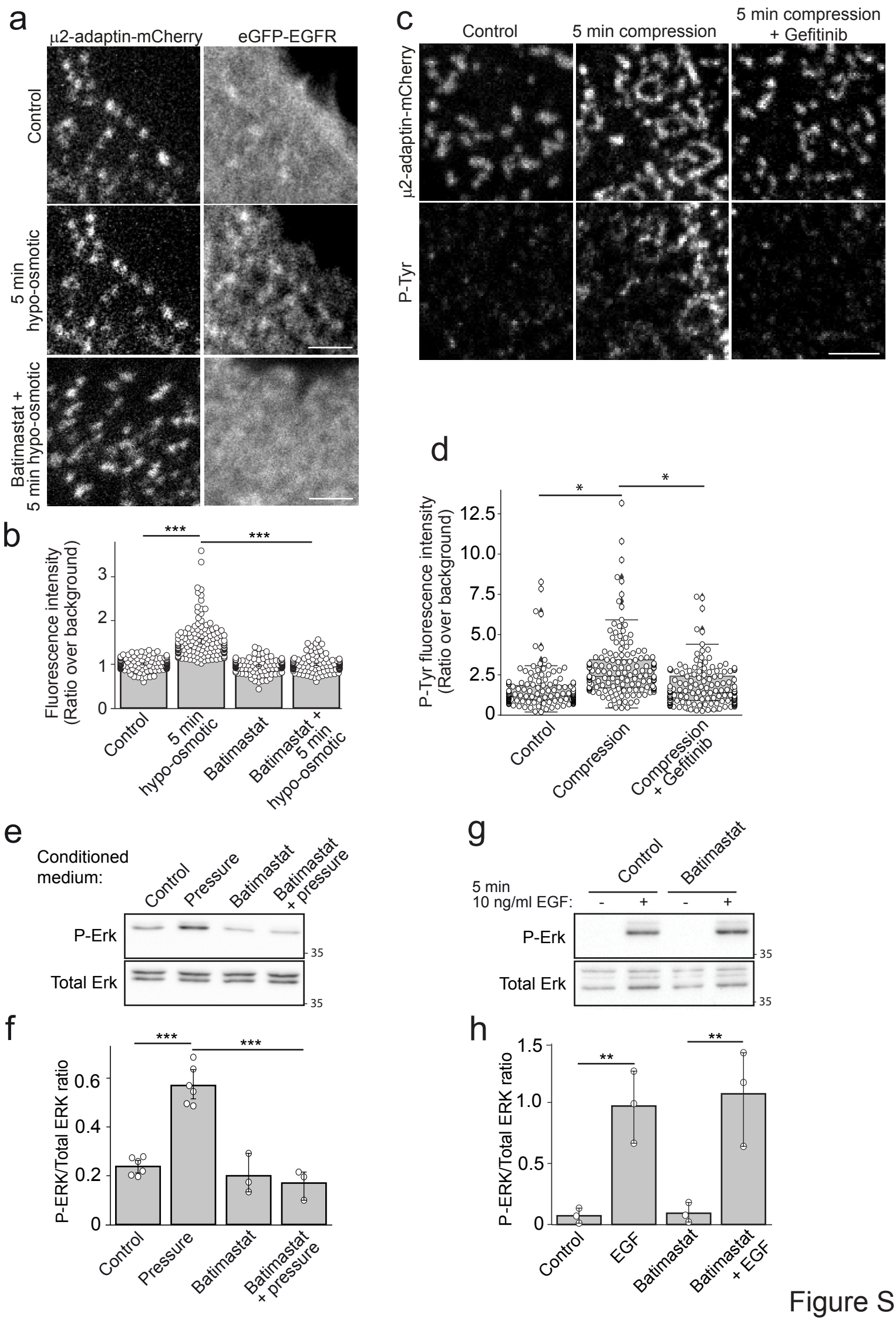
a
μ2-adaptin-mCherry
eGFP-EGFR
Control
5 min hypo-osmotic
Batimastat + 5 min hypo-osmotic
b
Fluorescence intensity (Ratio over background)
***
***
Control
5 min hypo-osmotic
Batimastat
Batimastat + 5 min hypo-osmotic
c
Control
5 min compression
5 min compression + Gefitinib
μ2-adaptin-mCherry
P-Tyr
d
P-Tyr fluorescence intensity (Ratio over background)
*
*
Control
Compression
Compression + Gefitinib
e
Conditioned medium:
Control
Pressure
Batimastat
Batimastat + pressure
P-Erk
Total Erk
35
f
P-ERK/Total ERK ratio
***
***
Control
Pressure
Batimastat
Batimastat + pressure
g
Control
Batimastat
5 min
10 ng/ml EGF:
P-Erk
Total Erk
35
h
P-ERK/Total ERK ratio
**
**
Control
EGF
Batimastat
Batimastat + EGF

Figure S3

Figure S3. **Characterization of EGFR activation modalities under compression. a**, Genome-edited HeLa cells expressing endogenous mCherry-tagged μ2-adaptin were transfected with a plasmid encoding eGFP-tagged EGFR, seeded on glass, serum-starved for 2 h, subjected to hypo-osmotic shock (90% water) in the presence or not of Batimastat and imaged by TIRF microscopy every 10s for 20 min. Scale bar: 2.5 μm. **b**, Quantification of eGFP-EGFR enrichment at CCSs before or 5 min after hypo-osmotic shock in cells treated as in a and showing some degree of EGFR recruitment at CCSs (*** $P<0.001$, two tailed paired Student's T-test; 50 structures per experiment in three independent experiments were analysed). **c**, Genome-edited HeLa cells expressing endogenous mCherry-tagged μ2-adaptin were serum starved for 2 h, treated with 10 μM Gefitinib or vehicle for 1 h and subjected or not to compression. Cells were fixed after 5 min of compression, without releasing compression. An immunostaining against phosphorylated tyrosines (P-Tyr) was then performed. Scale bar: 2.5 μm. **d**, Quantification of P-Tyr enrichment at CCSs before (control) or 5 min after compression in cells treated as in e (* $P<0.05$, Kruskal-Wallis One Way analysis of variance on ranks; 50 structures per experiment in three independent experiments were analysed). **e**, Western-blot analysis of phospho-ERK (P-ERK) levels in HeLa cells serum starved for 2 h, and treated for 5 min with conditioned medium from uncompressed cells (control and Batimastat conditions) or from cells compressed for 5 min in the presence or not of Batimastat (pressure and pressure + Batimastat conditions). **f**, Densitometry analysis of bands obtained in Western-blots as in e. Results are expressed as mean ratio of P-ERK/total ERK ± SD from three independent experiments **(**two tailed paired Student's T-test) **g**, Western-blot analysis of phospho-ERK (P-ERK) levels in HeLa cells serum starved for 2 h, treated or not with Batimastat for 1 h, and stimulated with 10 ng/ml EGF or not as indicated (representative image of three independent experiments). Total-ERK was used as loading control. **h**, Densitometry analysis of

bands obtained in Western-blots as in g. Results are expressed as mean ratio of P-ERK/total ERK ± SD from three independent experiments (** $P<0.01$, One Way Analysis of Variance – ANOVA, Student-Newman-Keuls).

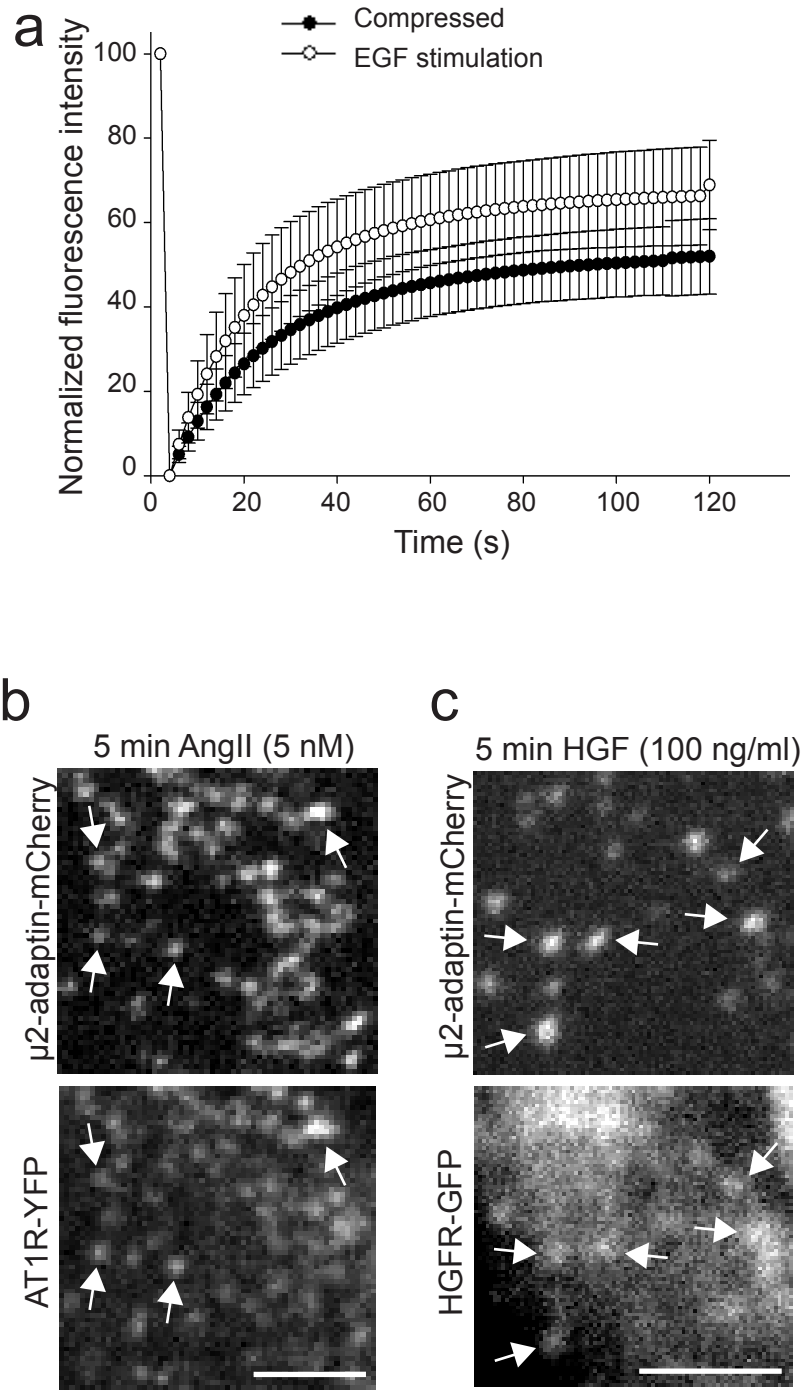
a
Compressed
EGF stimulation
Normalized fluorescence intensity
100
80
60
40
20
0
0
20
40
60
80
100
120
Time (s)
b
5 min AngII (5 nM)
μ2-adaptin-mCherry
AT1R-YFP
c
5 min HGF (100 ng/ml)
μ2-adaptin-mCherry
HGFR-GFP

Figure S4

Figure S4. **Alteration of receptor sorting and dynamics under compression. a**, Quantification of fluorescence recovery after photobleaching of eGFP-EGFR fluorescence in individual CCSs in cells stimulated with EGF or compressed under an agarose plug, as indicated. All results are expressed as mean ± SD. **b**, Genome-edited HeLa cells expressing endogenous mCherry-tagged μ2-adaptin were transfected with a plasmid encoding YFP-tagged AT1R. Cells were serum-starved for 2 h, stimulated with 5 nM Angiotensin II for 5 min and imaged by TIRF microscopy every 10s for 20 min. Scale bar: 2.5 μm. **c**, Genome-edited HeLa cells expressing endogenous mCherry-tagged μ2-adaptin were transfected with a plasmid encoding GFP-tagged HGFR. Cells were serum-starved for 2 h, stimulated with HGF (100 ng/ml) for 5 min and imaged by TIRF microscopy every 10 s for 20 min. Scale bar: 2.5 μm.

Supplementary Videos

Video 1. **EGFR recruitment to CCSs.** Genome-edited HeLa cells expressing endogenous mCherry-tagged μ2-adaptin were transfected with a plasmid encoding eGFP-tagged EGFR, seeded on glass and starved for 2 h. Cells were then compressed under an agarose plug (1 kPa pressure) and imaged by TIRF microscopy every 15s for 30 min. Scale bar: 10 μm.

Video 2. **EGFR recruitment to CCSs in the presence of Gefitinib or Batimastat.** Genome-edited HeLa cells expressing endogenous mCherry-tagged μ2-adaptin were transfected with a plasmid encoding eGFP-tagged EGFR, seeded on glass, starved for 2 h and treated with 10 μM Gefitinib (left) or 10 μM Batimastat (right). Cells were then compressed under an agarose plug (1 kPa pressure) and imaged by TIRF microscopy every 15 s for 30 min. Scale bar: 10 μm.

Video 3. **TfR is lost from CCSs upon compression.** Genome-edited HeLa cells expressing endogenous GFP-tagged μ2-adaptin were transfected with a plasmid encoding mCherry-tagged TfR, seeded on glass, then compressed under an agarose plug (1 kPa pressure) and imaged by TIRF microscopy every 10 s for 30 min. Scale bar: 5 μm.